

HOLLAND & HART^{LLP}
ATTORNEYS AT LAW

DENVER • ASPEN
BOULDER • COLORADO SPRINGS
DENVER TECH CENTER
BILLINGS • BOISE
CHEYENNE • JACKSON HOLE
SALT LAKE CITY • SANTA FE
WASHINGTON, D.C.

P.O. BOX 2208
SANTA FE, NEW MEXICO 87504-2208
110 NORTH GUADALUPE, SUITE 1
SANTA FE, NEW MEXICO 87501-6525

TELEPHONE (505) 988-4421
FACSIMILE (505) 983-6043

William F. Carr

wcarr@hollandhart.com

August 27, 2003

VIA HAND DELIVERY

David R. Catanach
Hearing Examiner
Oil Conservation Division
New Mexico Department of Energy,
Minerals and Natural Resources
1220 South Saint Francis Drive
Santa Fe, New Mexico 87505

RECEIVED

AUG 27 2003

Oil Conservation Division

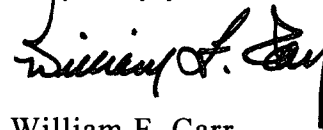
Re: Case No. 13121: Application of Benson-Montin-Greer Drilling Corp. for qualification of certain acreage within the East Puerto Chiquito Mancos Unit for the Recovered Oil Tax Rate pursuant to the New Mexico Enhanced Oil Recovery Act, Rio Arriba County.

Dear Mr. Catanach:

Enclosed is the information you requested be supplied by Benson-Montin-Greer Drilling Corporation at the August 21, 2003 examiner hearing on the above-referenced application. This data explains the proposed injection of soda ash and surfactant into the subject reservoir.

If you need anything further from Benson-Montin-Greer Drilling Corp. for your consideration of this application, please advise.

Very truly yours,



William F. Carr

Enclosure

cc: Mr. Jim Hornbeck
Benson-Montin-Greer Drilling Corp.
4900 College Blvd.
Farmington, New Mexico 87402

SURTEK, INC.

1511 Washington Avenue -- Golden, Colorado 80401 -- (303)278-0877 -- FAX (303)278-2245

Facsimile Transmittal Advisory

Date: 3/25/03
Deliver To: AL GREER
Company Name:
FAX Number: 505-327-9207
Phone Number:

From: HARRY SURKALO

COPY

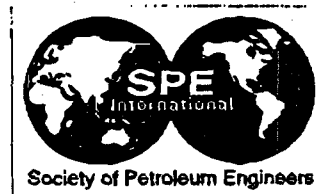
Total number of pages in FAX (including this cover sheet): 12

AL

THIS FAX CONTAINS:

- (1) 8 PAGE PAPER ON CAMBRIDGE ASP PROJECT
PAGE 4 & 5 OF THIS PAPER TALKS ABOUT
HANDLING OF CHEMICALS
- (2) 2 PAGES SCHEMATIC OF SODA ASH IND. PLANT
FROM ABOVE PAPER
- (3) 1 PAGE SCHEMATIC USING SODIUM HYDROXIDE

The information in this facsimile transmission is CONFIDENTIAL AND LEGALLY PRIVILEGED, and is intended only for the use of the individual or entity named above. If you are not the intended recipient, or an employee or agent responsible to deliver it to that recipient, you are hereby notified you have received this transmission in error and any disclosure, copying, distribution, or action taken in reliance on the contents of this transmission is prohibited. If you have received this transmission in error, please immediately notify us by telephone, and return the original message to us at the above address via the U.S. postal service. Thank you.



SPE 55633

Alkaline-Surfactant-Polymer Flooding of the Cambridge Minnelusa Field

Jay Vargo, Jim Turner, Barrett Resources, Bob Vergnani, Coleman Oil and Gas, Malcolm J. Pitts, Kon Wyatt, Harry Surkalo, Surtek, and David Patterson, Unichem

Copyright 1999, Society of Petroleum Engineers Inc.

This paper was prepared for presentation at the 1999 SPE Rocky Mountain Regional Meeting held in Gillette, Wyoming, 15-18 May 1999.

This paper was selected for presentation by an SPE Program Committee following review of information contained in an abstract submitted by the author(s). Contents of the paper, as presented, have not been reviewed by the Society of Petroleum Engineers and are subject to correction by the author(s). The material, as presented, does not necessarily reflect any position of the Society of Petroleum Engineers, its officers, or members. Papers presented at SPE meetings are subject to publication review by Editorial Committees of the Society of Petroleum Engineers. Electronic reproduction, distribution, or storage of any part of this paper for commercial purposes without the written consent of the Society of Petroleum Engineers is prohibited. Permission to reproduce in print is restricted to an abstract of not more than 300 words; illustrations may not be copied. The abstract must contain conspicuous acknowledgment of where and by whom the paper was presented. Write Librarian, SPE, P.O. Box 833836, Richardson, TX 75083-3836, U.S.A., fax 01-972-952-9435.

Abstract

Many factors were responsible making the Cambridge Minnelusa Field alkaline-surfactant-polymer flood a technical and economic success, producing 1,143,000 bbls of incremental oil at a cost of \$2.42 per barrel. A thorough understanding of the reservoir from reservoir engineering and geologic studies, as well as a promising laboratory injected fluid design unique to the reservoir water, oil, and rock were the initial key factors for deciding field implementation. Facilities were designed for proper mixing and injection of the specified chemical solution. Collection of oil, water, and chemical production information was critical to interpreting the project performance. Field operations and solving day to day issues were important for success. The paper objective is to discuss project performance and factors making the Cambridge alkaline-surfactant-polymer flood successful.

The laboratory study formulated an injected alkaline-surfactant-polymer solution of 1.25 wt% sodium carbonate plus 0.1 wt% active Petrostep B-100 plus 1450 mg/L Alcoflood 1275A followed by a polymer mobility control buffer solution. Beginning in January 1993, 30.7% V_p of alkaline-surfactant-polymer solution was injected immediately after primary production. Mobility control buffer polymer solution started in September 1996. Water flush began in May 2000.

The Cambridge Minnelusa reservoir estimated ultimate oil recovery is 60.9% OOIP from the swept area. Numerical simulation waterflood prediction was 32.8% OOIP of the swept area. Initial water breakthrough occurred at 20% V_p of fluid injection instead of 5% V_p typically seen in Minnelusa

waterfloods. Estimated ultimate incremental oil production from the swept area is 28.1% OOIP. Oil recovery through April 2000 is 48.4% OOIP of the swept area with an oil cut of 20%. Up to 600 mg/L polymer was produced in three of six production wells. Traces of surfactant was observed, but no alkali has been noted.

Field operations were designed to maximize project economics. Production facilities were consolidated. All producing wells used rod pumps. Injection facilities were simple, but capable of mixing chemicals at design concentrations and injecting the solution at the targeted rates. Injection and produced water qualities were monitored to maximize alkali-surfactant-polymer oil recovery and to reduce operating expenses.

Introduction

The purpose of the alkaline-surfactant-polymer technology is to produce incremental oil by reducing the waterflood residual oil saturation. The technology combines interfacial tension reducing chemicals (alkali and surfactant) with a mobility control chemical (polymer). The interfacial tension reducing chemicals minimize the capillary forces that trap waterflood residual oil while the mobility control chemical improves reservoir contact and flood efficiency. The first alkaline-surfactant-polymer project was performed in a nearby Minnelusa field.^{1,2} Other alkaline-surfactant-polymer projects include a pilot in an Oklahoma field,³ and three in Peoples Republic of China oil fields.^{4,5,6,7,8,9} Lessons learned from these projects and applied to the Cambridge alkaline-surfactant-polymer project are: 1) good mobility control is essential for a successful project, 2) a detailed study of the reservoir including geology, reservoir engineering, laboratory

fluid design, and numerical simulation improve the probability of success, 3) injection facilities must mix the injected solution according to the design parameters for a successful project, and 4) attention to detail including quality control of injected materials and scheduled maintenance of injection and mixing equipment is important.

The Cambridge Field, located in Section 28 of Township 53N and Range 68W in Crook County, Wyoming, is operated by Plains Petroleum Operating Company, a subsidiary of Barrett Resources Corp. The field produces 31 cp, 20° API gravity crude oil from the Permian Minnelusa Upper "B" sand at 2,139 m (7,108 ft). The reservoir temperature is 55.6°C (132°F) and the average thickness is 8.75 m (28.7 ft). Crude oil formation volume factor is 1.03 with a bubble point of 586 kPa (85 psi). Average porosity and permeability are 18% and $0.834 \mu\text{m}^2$ (845 md), respectively. Connate water saturation was 31.6% with an initial reservoir pressure of 12,355 kPa (1792 psi).

Field History

The Cambridge Field is defined as 1,131,500 m³ (7,117 Mbbl) pore volume with 795,000 STm³ (4,875 MSTB) of original oil in place. The field was discovered by McAdams, Roux and Associates in 1989 with the MRA Federal 31-28. All subsequent drilling locations were based on 3-D seismic data. Peak primary oil production was 77.7 m³/day (489 BOPD). Within a year, the production rate declined to 5.9 m³/day (37 BOPD) as is typical of Minnelusa reservoirs. The producing mechanism is fluid and rock expansion with the initial GOR being essentially zero. The Federal 21-28 and 32-28 began production in June 1990 with peak production of 11.0 and 46.4 m³/day (69 and 292 BOPD), respectively. Federal 23-28 started production in October 1990 with peak production occurring in November 1990 of 33.7 m³/day (212 BOPD) of oil and 2.9 m³/day (18 BWPD) of water.

Primary production was 34,600 m³ (217.7 Mbbls) oil and 3,800 m³ (23.3 Mbbls) water from December 1989 to January 1993.

Water injection began in January 1993 with the conversion of the Federal 32-28. Alkaline-surfactant-polymer solution injection started one month later in February 1993. Therefore, the alkaline-surfactant-polymer process was applied as a secondary flood. As result, operating costs are not duplicated by running a waterflood followed by an alkaline-surfactant-polymer flood. The polymer drive solution began injection in October 1996 with the final water drive began in May 2000. The chemical injection sequence was: 30.7% V_p of alkaline-surfactant-polymer solution followed by 29.7% V_p of polymer drive solution followed by water to the economic limit. Percent pore volume is based on swept area pore volume. Swept area is defined as the volume of reservoir contacted by the injected fluid and is approximately 82% of the total pore volume for the Cambridge Field. Swept area injected volume and oil recovery calculations are more comparable to radial coreflood results than total field values. For reservoirs like the Minnelusa in which well placement is limited by reservoir geometry, comparison of total field calculations can be misleading. Differences in total field calculations are often dictated by reservoir contact inefficiency and not process efficiency. When this condition exists, swept area calculation is a better comparison to delineate accurately the economic injected chemical volumes and oil recovery.¹⁰ Calculated swept area pore volume is 926,400 m³ (5,827 Mbbl) and the original oil in place is 647,300 m³ (4,071.8 Mbbl).

Interpretation of 3-D seismic data resulted in the drilling of the Federal 41A-28 in November 1994 and the Federal 33-28 in February 1996. Federal 41A-28 was produced through March 1996 and Federal 33-28 was produced through October 1998.

Geologic Description

The Cambridge Field is on the eastern flank of the Powder River Basin and produces oil from the Permian Minnelusa Upper "B" sandstone. The Minnelusa formation is unconformably overlain in this area by the Opeche siltstone member of the Permian Goose Egg formation, which in turn is overlain by the regional Minnekahta Limestone, also a member of the Goose Egg formation. The Minnelusa vertical sequence consists of alternating carbonates and sandstones.

The Minnelusa Upper "B" reservoir is a friable, Eolian sandstone with modest amounts of dolomite and anhydrite cement and is a preserved remnant of a highly dissected coastal dune complex. Dolomite and anhydrite cement are the main chemical adsorbing sites of the Cambridge sand. Fig 1. depicts the field's net pay isopach. The reservoir dips approximately 1.7° to the southwest. A water-oil contact controls the field's producing limit on the southwest. Dystra-Parsons is 0.57. Preferential flow of injected fluids follows an axis along wells 41A-28 and 21-28. The 3-D seismic indicates the sand thins between wells 33-28 and 23-28.

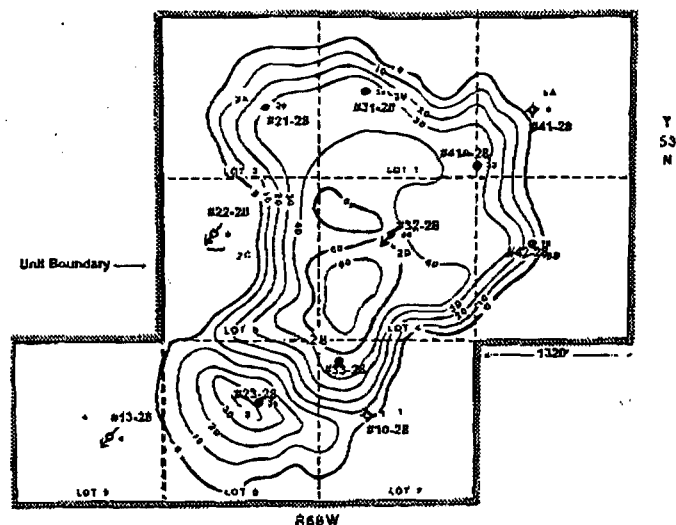


Figure 1 Cambridge Field net pay isopach in feet.

The trapping mechanism at the Cambridge Field is stratigraphic, and results from the total encasement of the Upper "B" reservoir sand by the impermeable Opeche siltstone above and the impermeable Upper "B" Dolomite below. The Upper "B" Dolomite serves as the bottom seal for the oil accumulation as it rises stratigraphically over the laterally thickening Lower "B" sand. The Lower "B" sand is Eolian in origin and its surface has considerable topographic relief. The Upper "B" Dolomite was deposited on this pre-existing surface, thereby preserving its topography. During the next cycle of Eolian deposition, the Upper "B" sand accumulated and was preferentially preserved in the topographic lows of the underlying surface. The Upper "B" sand thins and ultimately pinches out as it rises laterally away from the topographic low and up against the thick adjacent Lower "B" sand. The Upper "B" Dolomite, rising stratigraphically in the same manner, ultimately juxtaposes the Opeche siltstone, thereby completely encasing the Upper "B" sand within the impermeable strata.

Alkaline-Surfactant-Polymer System Design

Laboratory Studies - Extensive laboratory design and testing were performed to reduce the risk of field application. Several alkaline-surfactant-polymer formulations were found that provided ultra-low interfacial tension and optimal phase behavior using surfactant concentrations of 0.1 wt% active. Fig. 2 shows the effect on the interfacial tension of the surfactant plus varying concentrations of sodium carbonate. Low interfacial tension between the 0.1 wt% active surfactant plus sodium carbonate solutions and Cambridge crude oil on the order of 10^{-3} mN/m were obtained for alkali concentrations from 0.75 to 2.0 wt%.

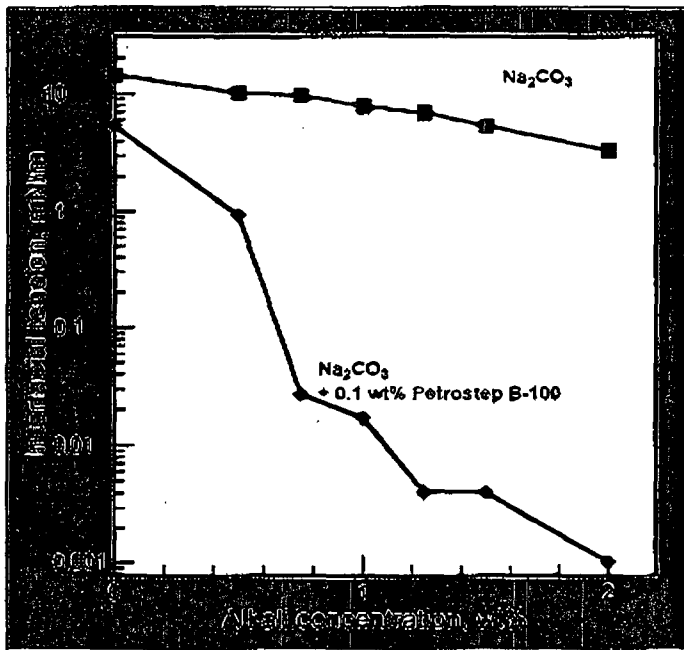


Figure 2 Interfacial tension of 0.1 wt% active Petrostep B-100 plus Na_2CO_3 at varying alkali concentrations

Bench top viscosity studies and linear corefloods were used to determine the rheologic properties of the polymer solution and the concentration of polyacrylamide polymer required to provide a unit mobility ratio for aqueous solutions displacing crude oil.¹¹ Linear and radial coreflood tests indicated that the mobility ratio for water displacing the crude oil ranged from 2.2 to 5.8, which is unfavorable. A low interfacial tension flood reduces the residual oil saturation causing the water phase to become more mobile as dictated by relative permeability. The increased effective water permeability exacerbates viscous fingering. Therefore, polymer is essential. In radial corefloods, water breakthrough was observed by 0.10 pore volumes of water injection and water cuts of more than 98% occurred with less than 37% OOIP recovered. The average waterflood recovery from five radial corefloods was 44.3% OOIP after injection of an average of 3.0 pore volumes of water and oil cuts of 2% or less. The high mobility ratio and early water breakthrough indicated that polymer is required.

Radial corefloods measured the oil recovery performance using field proportioned pore volumes of injected chemicals. Radial corefloods were sandpacks using fresh unconsolidated core from well Plains Federal 23-28. Dimensions of the sandpacks were 5.04 cm (2 inches) high by 15.24 cm (6 inches) in diameter. Fluid injection was into a 1/8 inch ID perforated tubing located in the center of the sand disc. Injected fluid sequence was 3 V_p of water, 0.3 V_p of alkaline-surfactant-polymer solution, 0.3 V_p of polymer solution, followed by 1 to 1.5 V_p of water. Fig. 3 shows the oil recovery and water cut during the radial coreflood of the alkaline-surfactant-polymer solution ultimately injected into the field. The chemical combination injected into the field was 1.25 wt% Na_2CO_3 plus 0.1 wt% active Petrostep B-100 plus 1475

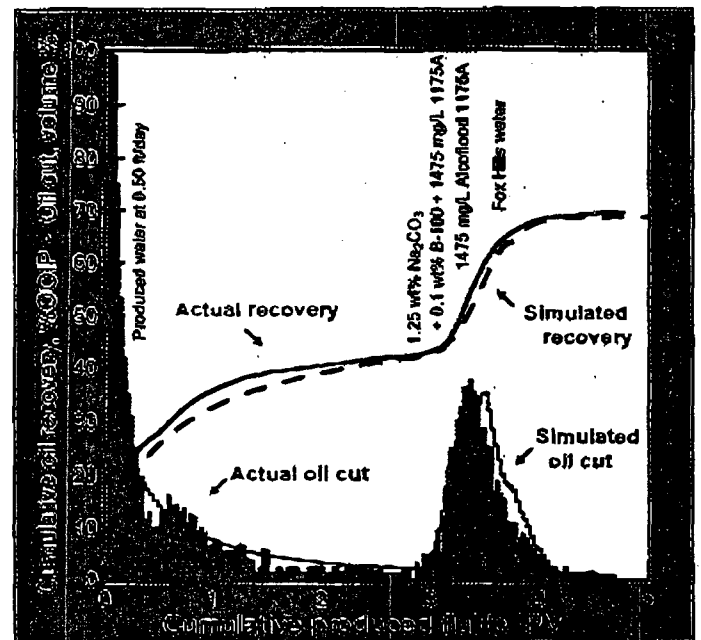


Figure 3 Cambridge radial coreflood with Petrostep B-100 plus Na_2CO_3 plus Alcoflood 1175A

mg/L Alcoflood 1175A. Water for chemical dissolution in the laboratory study and the field application was Fox Hills water which is a 1400 mg/L TDS water that is essentially a 50:50 mixture of sodium sulfate and sodium carbonate with less than 10 mg/L hardness. The alkaline-surfactant-polymer injection sequence increased the oil cut by as much as 36 percentage points and improved the recovery by 27% OOIP. Alkaline-surfactant-polymer flood produced 65% more oil than a waterflood. Coreflood waterflood represents field primary plus waterflood performance. Average initial oil saturation of the radial corefloods was $0.731 V_p$ with the average waterflood residual oil saturation being $0.402 V_p$. Final oil saturation after chemical was $0.186 V_p$.

Injection pressures during coreflooding increased by 85% during alkaline-surfactant-polymer injection at constant injection rate. The residual pressure after water-flushing was 28% greater than during the waterflood indicating effective water permeability reduction that would help divert fluids and improve sweep efficiency. Corefloods were constant rate with the pressure dictated by core permeability to the injected fluid.

Numerical Simulation - Numerical simulation for waterflood and chemical flooding was performed using the GCOMP simulation package. Its black oil option includes capabilities for incorporating chemical flooding properties such as: interfacial tension reduction by alkali and surfactant, effect of water salinity on interfacial tension, capillary number and relative permeability effects from reduced interfacial tension, polymer viscosity and residual resistance factor, chemical consumption by reservoir rock, and chemical partitioning. The chemical option was calibrated by history matching the performance of radial corefloods. Polymer rheology input data was from the linear corefloods that had three concentrations of polymer injected at three different injection or shear rates. Two sequences of polymer were injected in the linear corefloods, one with polymer dissolved in the alkaline-surfactant solution and the second in fresh water. Adsorption isotherms were developed from linear and radial coreflood effluent analysis. Alkali, surfactant, and polymer limiting adsorption values were 0.076, 0.004, and 0.017 g/100 g sand. Fig. 3 shows the radial coreflood oil recovery history match. Chemical production and differential pressure were history matched also. Due to the greater fluid exiting surface area of the radial core, capillary end effects are larger for radial corefloods making the oil prediction more pessimistic. Capillary end effects of radial corefloods were accounted for by matching the pressure history. Pressure differential over length of the radial corefloods were of similar magnitude as the field, 5 psi/ft for the field and 8 psi/ft for the radial corefloods.

The field numerical simulation consisted of a 14 by 21 grid with three layers. Areal dimension of each grid block is 1.4 acres. History match is through June 1992, before fluid injection. Numerical simulation waterflood prediction to an oil cut of 5% was 220,700 m³ (1,388 MSTB) oil or 28.5% OOIP of the total

reservoir. Waterflood oil prediction from the swept area is 212,600 m³ (1,337 MSTB) or 32.8% of its OOIP. Total water injection was 1,368,200 m³ (8,606 Mbbl). The alkaline-surfactant-polymer flood forecast to a 5% oil cut was 363,900 m³ (2,289 MSTB) oil or 56.2% OOIP from the swept area and 47.0% OOIP of the total reservoir. Incremental oil prediction was 130,600 m³ (901 MSTB) or 22.1% OOIP of the swept area. This oil, representing 65% of the waterflood plus primary recovery, is produced two years earlier than that for the waterflood, a 10% decrease in project life.

Alkaline-Surfactant-Polymer Facilities and Operation

The injection plant, mixing facilities, artificial lift, and produced fluid handling were based on simplicity and dependability. The Cambridge alkaline-surfactant-polymer injection plant was divided into two parts: a chemical injection portion and a produced water disposal portion. Fig. 4 is a schematic of the Cambridge injection plant. Plant design parameters were 20,675 kPa (3000 psi) capacity, 238.4 m³ (1,500 bbls) per day ASP solution injection rate, 159.0 m³ (1,000 bbls) per day produced water disposal injection rate, and 40 to 45 days of chemical storage. The plant was designed to minimize operator attention. Once the plant was running, required operator time was one hour or less per day.

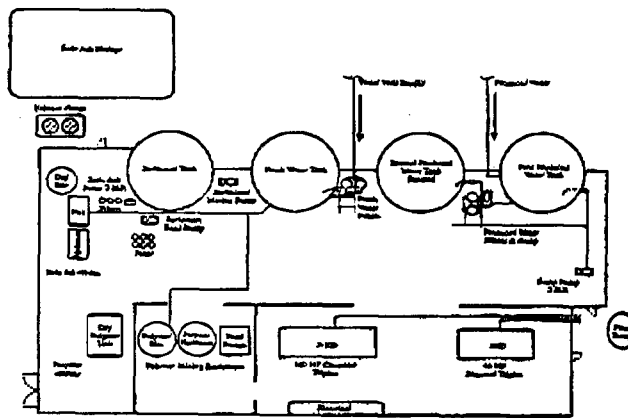


Figure 4 Cambridge Field injection plant facilities schematic

Alkali Mixing - Sodium carbonate (soda ash) handling equipment consisted of a horizontal long term storage vessel, a vertical day silo, two mix tanks, a hydration tank, a transfer pump, and a set of filters. Sodium carbonate was received in 22,680 kg (50,000 lbm) shipments that were pneumatically transferred to the long term storage vessel. The day silo was filled pneumatically with a 40-hp 550 CFM blower from the long term storage vessel. The day silo was equipped with a high level shut down switch to prevent over flow. In both cases, exhaust air was filtered through a dust collector. The day silo also was equipped with a vibrating bin activator, a manual slide gate, a low-level shut down switch, a clean out manway, an inspection hatch, an inlet diffuser, and an exhaust line. Approximately

2,980 kg (6,600 lbm) of sodium carbonate was mixed with 132 m³ (830 bbls) per day water by dropping the alkali into a mixing vessel using a DC motor drive variable speed auger. Mix tank temperature was 16.1°C (61°F). The solution was stirred with a 1/3 hp 1750 rpm mixer. Fox Hills water did not require softening to dissolve alkali. Sodium carbonate quality control and equipment maintenance were important.

Surfactant Mixing - Surfactant was stored in an internally epoxy coated, insulated 63.6 m³ (400 bbl) steel tank. Surfactant was maintained at 32 to 38°C (90 to 100°F). Surfactant shipments of approximately 23.8 m³ (150 bbls) were diluted with 15.9 m³ (100 bbls) of water immediately upon receipt to reduce the raw surfactant viscosity. A proportioning pump transferred 0.5 to 0.6 m³ (3 to 4 bbls) of diluted surfactant per day to the sodium carbonate mix tank. The sodium carbonate plus surfactant solution was transferred from the mix tank to a second mix tank and stirred for 5 to 10 minutes with a 1/3 hp 1750 rpm mixer. Surfactant was easy to store, mix, and handle.

Polymer Mixing - Polymer handling and mixing were straightforward. Dry polymer in 25 kg (55 lbm) bags were dumped daily into the polymer mixing bin. From the mixing bin, the polymer was fed through an eductor. The eductor wetted each grain of polymer as the mix tank was filled. From the mix tank, polymer was transferred to a hydration tank to allow additional time for the polymer molecule to be completely wetted. From the hydration tank, the polymer solution was pumped into the sodium carbonate-surfactant injection stream. A programmable logic controller governed mixing volumes and rate. All equipment was low shear to prevent polymer degradation. Progressive cavity pumps were used to transfer polymer solution and a slow speed impeller mixer stirred the mix tank. Equipment maintenance was important for dependable, precise polymer mixing.

Quality Control - Quality control for each chemical was important. Easily accessible sample points in the mixing process allowed checks of the mixed solution at different stages. Injected fluid samples were collected for detailed laboratory analysis. Gross checks were performed monthly using chemical stock and delivery amounts.

Filtration - Fox Hills water for chemical dissolution and the concentrated sodium carbonate-surfactant injection stream was 1 micron filtered. The alkaline-surfactant-polymer solution was 25 micron filtered. All filters were nominal bag filters and were equipped with a backup filter and high pressure kill switches. An actuator valve automatically diverted flow to the backup filter if pressures exceeded design specifications.

From the 25 micron filter, the alkaline-surfactant-polymer solution was fed into the low pressure side of the triplex pump. Suction lines were schedule 40, internally coated steel piping and discharge lines were schedule 80, internally coated, 5.08 cm

(2 inches) steel piping. The alkaline-surfactant-polymer injection well and produced water disposal well used 5.08 cm (2 inches) nominal, 20,685 kPa (3000 psi), 93.3°C (200°F), fiberglass pipe.

Alkaline-Surfactant-Polymer Flood Oil Production

Primary recovery to the start of flooding on January 22, 1993 amounted to 34,600 m³ oil (217.7 MSTB, ~ 4.5% OOIP) and 3,800 m³ water (23.8 MBW). Fig. 5 depicts the oil and water production. Primary oil production from the swept area is estimated to be 26,400 m³ (166.2 MSTB) or approximately 4.1% of its OOIP. All primary water production came from the Federal 23-28 located in the down-dip portion of the reservoir underlain by water. Subsequent drilling of the CMU 33-28 producer established that the field's water leg extended slightly to the north east of this location.

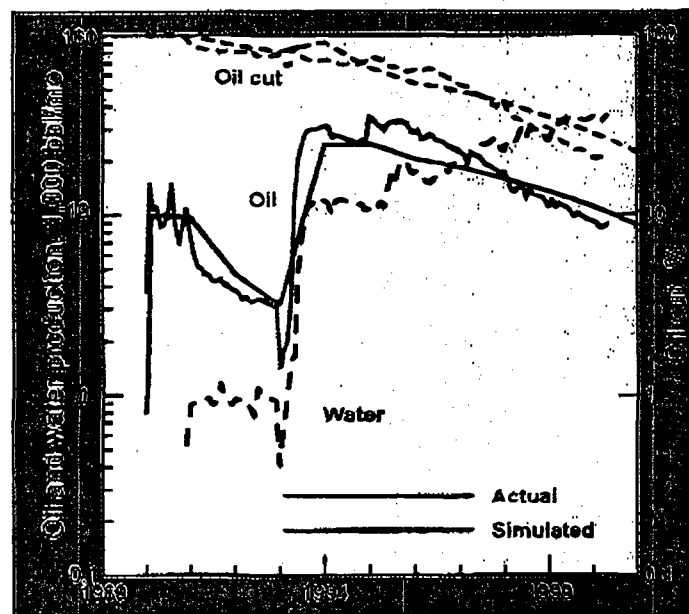


Figure 5 Cambridge Field actual and simulated oil and water production and oil cut

A total of 284,700 m³ (1,790 Mbbl) of ASP slug was injected into the Federal 32-28 well through the end of September 1996 when the polymer chase was initiated. This is approximately 25.2% of the total reservoir pore volume and 30.7% of that in the swept area. Total polymer drive injection was 277,653 m³ (1,746 Mbbl) bringing the total injection to 562,353 m³ (3,536 Mbbl) or 49.6% of the total pore volume and 60.4% of the swept-area pore volume. Water drive after polymer injection began on May 1, 2000.

Cumulative production through April 2000 was 321,632 m³ (2,023 MSTB) of oil and 282,721 m³ (1,778 MBBL) of water. An estimated 310,530 m³ (1,972 MSTB) of oil or 48.4% OOIP came from the swept area. Using decline-curve analysis and an estimated 5% oil-cut economic limit, the remaining reserves from January 1, 2000 are estimated to be 86,136 m³ (542 MSTB).

Total-field recovery is estimated to be 402,400 m³ (2,531 MSTB) of oil or approximately 52% of its OOIP. Within the swept area, the estimated-ultimate-recovery is expected to be 394,200 m³ (2,479.5 MSTB) of oil or 60.9% of its OOIP. Incremental oil is 181,700 m³ (1,143 MSTB) or 23.4% OOIP of the total field and 28.1% OOIP of the swept area. Injection/production balance is 0.95.

Produced Fluids

Production Facilities - Rod pumping is the preferred method of artificial lift for the Cambridge Field. Each pump was governed

with a stand alone computerized pump off controllers. Flowline pressure switches protect against over pressure and shut the well down if a leak is detected. Vibration and high tank kill switches are used to minimize problems. Flowlines and components of the fluid handling system are composites, polyethylene or internally coated steel. Down hole tubing and rod strings are carbon steel. Fig. 6 is a schematic of the production facilities including water knockout, flow splitter, treaters, produced water storage and treatment, gun barrel tank, and oil sales tank.

Handling - Treating of the Cambridge Field oil to meet pipeline specifications was no more difficult than treating oil produced from most other Minnelusa fields. CO₂, H₂S, and bacteria make the water corrosive. Produced polymer increased aqueous phase viscosity exacerbating separation. Use of large internally coated, treating vessels, gun barrel tank, and upstream chemical treatments reduced handling difficulties.

Chemical Analysis - Of the wells drilled before the start of the flood, only the Federal 31-28 has produced polymer. The Federal 33-28 and 41A-28 were placed into production thirty six and twenty four months, respectively, after alkaline-surfactant-polymer injection began. Both wells produced polymer immediately upon being placed on production. Fig. 7 depicts the produced polymer concentrations at the Federal 31-28. Chloride ion concentrations decline coincidentally with increasing polymer concentrations, indicating that Fox Hills or dissolution water is being produced. No polymer has been produced at the Federal 21-28 and 42-28 to the north or the Federal 23-28 to the south.

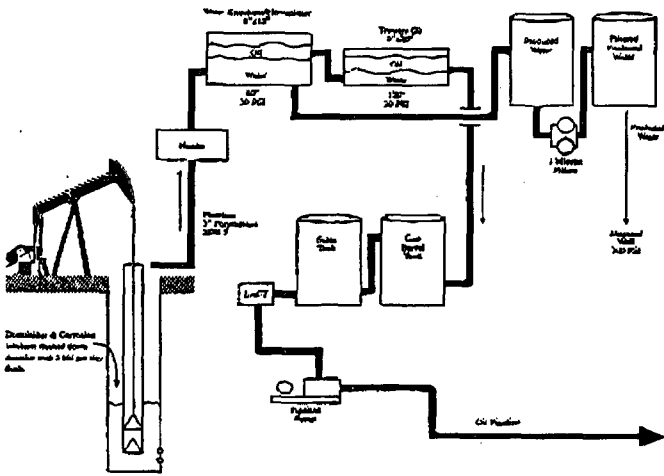


Figure 6 Cambridge production facilities schematic

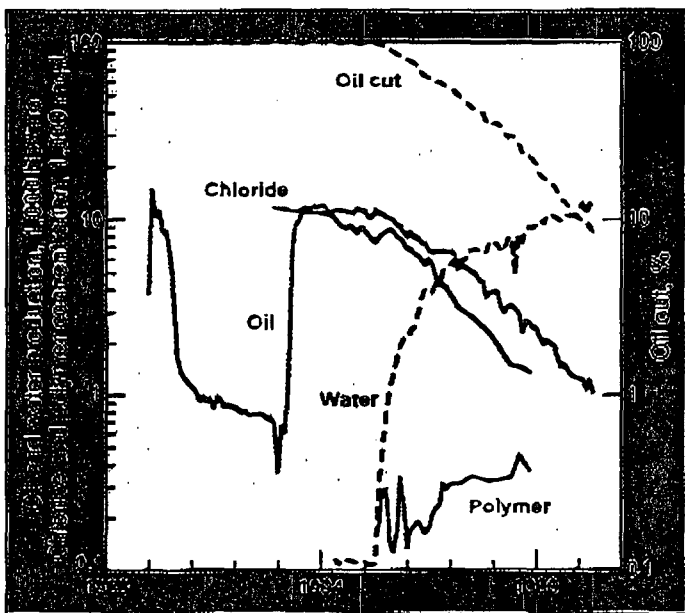


Figure 7 Well 31-28 produced polymer and chloride ion concentration, monthly oil and water, and oil cut

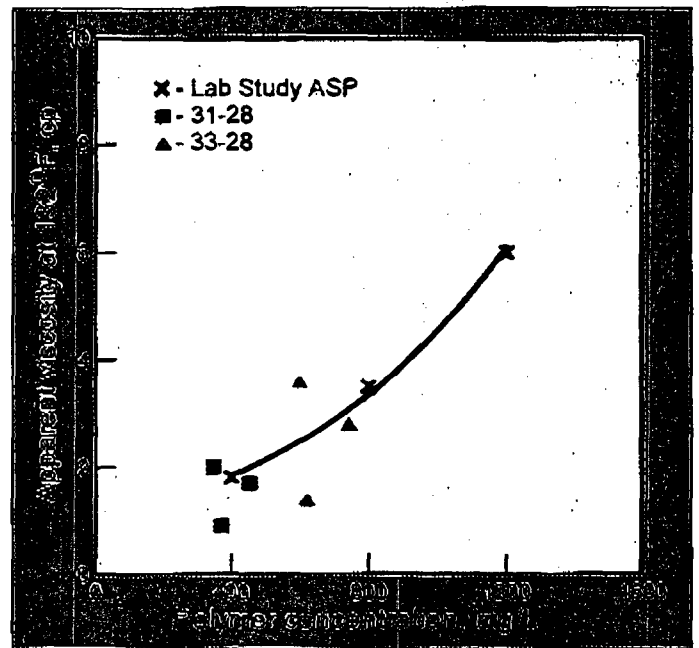


Figure 8 Brookfield viscosity (cp) of produced fluid samples and laboratory alkaline-surfactant-polymer solutions

Fig. 8 depicts the Brookfield viscosity of the produced fluids compared with the laboratory solutions. Produced fluid viscosi-

ties are essentially unchanged for similar total dissolved solids solutions. Produced surfactant concentrations have been detected at the Federal 31-28 and 33-28. However, the values are close to the methods detection limit of 50 mg/L and presence is erratic. No alkali production has been detected at any well.

Corrosion, Demulsification, and Bactericide Program

Up to 9% carbon dioxide in the produced fluids was the most significant contributor to production well failure. The Federal 31-28 was the most problematic well over the life of the project. From 1/92 to 4/94, bimonthly down hole treatments of a water-soluble corrosion inhibitor were performed at the Federal 23-28. Treatments were expanded to each well as water was produced. The corrosion inhibitor was changed to an oil soluble-highly water dispersible compound in 2/97 to provide better protection and the program was switched to continuous down hole injection behind the annulus.

Injection and produced water qualities were monitored for oxygen, sulfide, sulfate reducing bacteria, and oil carry over. Due to good mechanical facilities design and proper maintenance, oxygen intrusion has not been a problem. Oil carry over has varied over the life of the flood, appearing to increase with polymer production. Variation of residence times in the flow splitter, treaters, and produced water tanks helped reduce oil carry over.

Beginning January 1993, a general use demulsifier at 120 mg/L was continuously injected into the production well flow lines. During the early months of 1994, treater upsets and reject oil were experienced from emulsion pad buildups due to increasing oil and water production. In March 1994 demulsifier concentration was increased to 250 mg/L and treater temperatures increased from 48.9°C (120°F) to 60.0°C (140°F). Ultimately, a demulsifier specific for Cambridge was developed with continuous injection into the flow lines of the wells beginning in October 95. When polymer production began, a tight emulsion was produced which necessitated increasing the demulsifier concentration to 475 mg/L from 280 mg/L. Demulsifier was injected into the annulus of the production wells beginning November 96 providing longer treatment time which allowed a concentration reduction to 240 mg/L. In October 1998, further testing indicated that demulsifier concentration could be reduced to 90 mg/L and still have good oil and water separation at a lower heater treater temperature of 48.9°C (120°F).

Sulfate reducing bacteria, acid producing bacteria, and aerobic bacteria were evaluated for their role in corrosion, fowling of oil water separators, and plugging of the disposal well, the Federal 22-28. Initial bacterial remediation consisted of bimonthly glutaraldehyde treatments of the treaters and production wells beginning March 1993. When the flow splitter system was installed in November 1995, glutaraldehyde was replaced with a quaternary amine and treatment was shifted to a flow splitter.

Project Economics

Facilities costs beyond a typical Minnelusa waterflood plant were \$160,000. Included are chemical storage equipment, chemical mixing equipment, filtration, and labor for assembly. Total chemical cost was \$2,518,000. Incremental maintenance, electrical, and pumper costs were estimated at \$1,000 per month or \$89,000 for the total time chemical was injected. Total incremental cost is \$2,767,000. Cost per incremental barrel of oil is \$2.42.

Conclusions

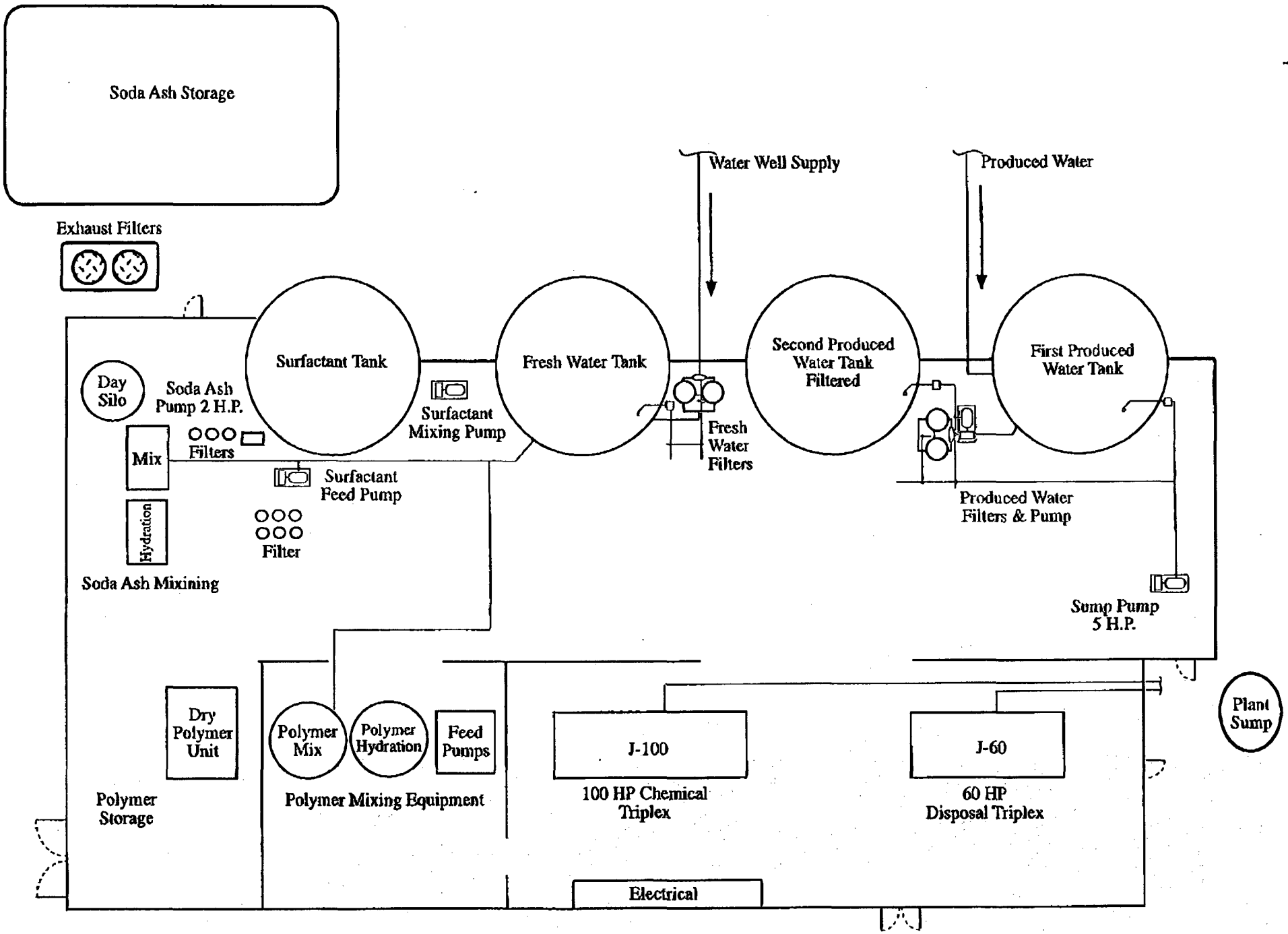
1. The alkaline-surfactant-polymer flood of the Cambridge Field ultimate oil production from the swept area is 60.9% OOIP compared with the numerical simulation waterflood prediction of 32.8% OOIP. Incremental alkaline-surfactant-polymer oil is determined to be 28.1% OOIP. Oil production as of April 2000 is 48.4% OOIP of the swept area with an oil cut of 20%.
2. A total of 1,143,000 bbls of incremental oil will be produced at a cost of \$2.42 per barrel.
3. Mixing and production facilities were kept simple with dependability as a key factor. Proper maintenance and quality control made mixing of the injected solution and treating of produced fluids no more difficult than a typical Minnelusa flood.
4. Reservoir engineering and geologic evaluation, a detailed laboratory injected fluid design, numerical simulation, facilities design and construction, and quality control of injected fluids were all important factors making the Cambridge Field alkaline-surfactant-polymer flood successful.

Acknowledgments

The authors thank Barrett Resources, Surtek and Unichem for permission to publish this paper. A special thanks to Kelly Dennis for field operations.

References

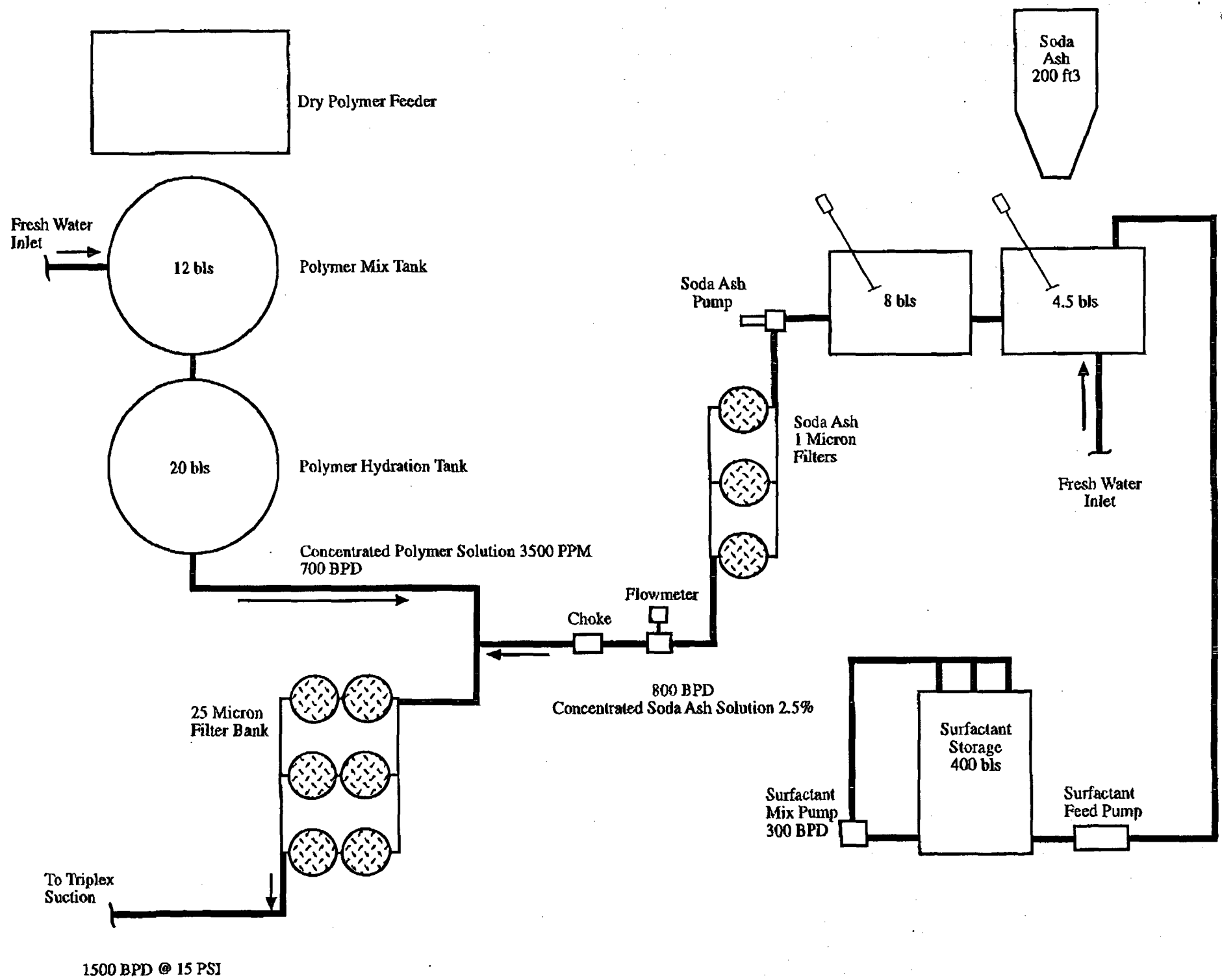
1. Clark, S.R., Pitts, M.J. and Smith, S.M.: "Design and Application of an Alkaline-Surfactant-Polymer Recovery System to the West Kiehl Field," SPE Advanced Technology Series, Vol. 1, No.1, Apr. 1993, p. 172-179.
2. Meyers, J., Pitts, M.J. and Wyatt, K.: "Alkaline-Surfactant-Polymer Flood of the West Kiehl Unit," SPE 24144, April 1992 presented at the DOE/SPE IOR Symposium in Tulsa, Ok.



#4004 P.010

SURTEK

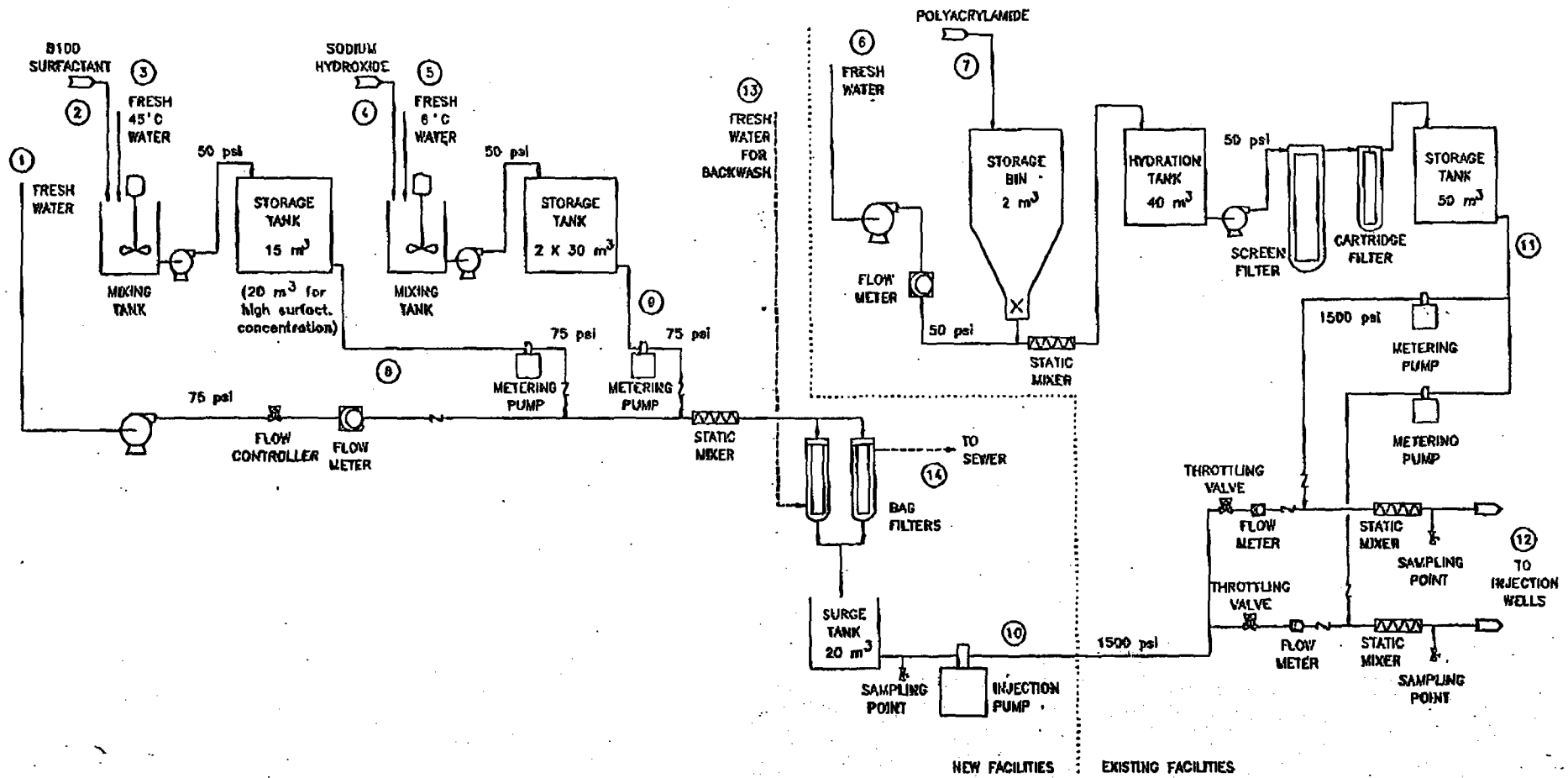
MAR.25'2003 14:24 303-278-2245



1500 BPD @ 15 PSI

FIGURE 1

ALKALI-SURFACTANT-POLYMER MIXING PLANT
PROCESS FLOW DIAGRAM
USING SODIUM HYDROXIDE



Surtek's Approach to Design of a Chemical System for Recovery of Incremental Oil

Increase oil recovery by:

- Improving oil displacement efficiency
- Improving vertical sweep efficiency
- Improving horizontal sweep efficiency

COPY

First by:

Understanding your oil reservoir from both geological and engineering considerations

Then by:

Determining reservoir rock-oil-water interactions with laboratory testing for interfacial tension, phase behavior, and phase stability; and ranking chemical systems for oil recovery efficiency based on extensive Surtek database

Next by:

Optimizing the chemical composition and defining rock-chemical compatibility in linear reservoir rock studies

And finally by:

Evaluating the best chemical solutions in radial corefloods to recommend an oil recovery system for field application

Reduce risk further by:

Numerically simulating laboratory results and applying to future field operation

All work is done with reservoir oil, water, and rock

ASP flooding produces incremental oil at moderate cost

COPY

Alkaline-surfactant-polymer flooding boosts recovery of original oil in place at prices competitive with finding and acquiring new reserves

Kon Wyatt, Malcolm Pitts, and Harry Surkalo, Surtek, Inc., Golden, Colorado

If asked for the best location for finding oil, many people would suggest the region in which they have the most experience. And they would be right, because oil will be found where it is already known to exist; however, producing it is another matter. About 60% of our oil resources cannot be produced by conventional means and is left in the ground when it becomes too expensive to produce. Meanwhile, new reserves are sought elsewhere, even though these abandoned resources represent more oil than has ever been produced.

However, in reservoirs that can be waterflooded, field-proven alkaline-surfactant-polymer (ASP) flooding technology can unlock some of the residual resources. ASP can boost incremental oil recovery of a known resource in a mature field by up to 30% of original oil in place (OOIP). Converting these resources into proved undeveloped reserves could be the best discovery most companies make in a year. Following is an analysis of several pilot and field applications of ASP flooding, including an overview of the economics and a discussion of how it works.

BASIC ECONOMICS

The economics of the process can be very compelling and depend upon the reservoir and how it was developed. Since this is a flooding process, residual oil must be mobilized from the injection wells to production wells. And since the injected solution costs from \$0.75 to \$1.60 per bbl,

the sooner the mobilized oil is recovered the greater the rate of return. Thus, high permeability reservoirs or those with tight well spacing are the most favorable. But generally speaking, if a pattern pore volume can be injected in 15 years or less, the incremental rate of return will be greater than 40%. ASP technology could result in incremental oil recoveries ranging from 0.12 to 0.20 pore volume, and costs for this oil of \$1.75 to \$4.15 per bbl. These costs are certainly competitive with finding or acquisition costs.

Most of the cost of an ASP process is associated with the chemicals. If the field is currently under waterflood, then the majority of operating costs are born by the waterflood since the operations are not significantly more complex or costly. Plant modifications are also relatively minor, requiring only tanks for storage of the three chemicals, pumps for their transfer, and mixing equipment. Thus, for a relatively small up-front investment for design and facilities, one is ready to

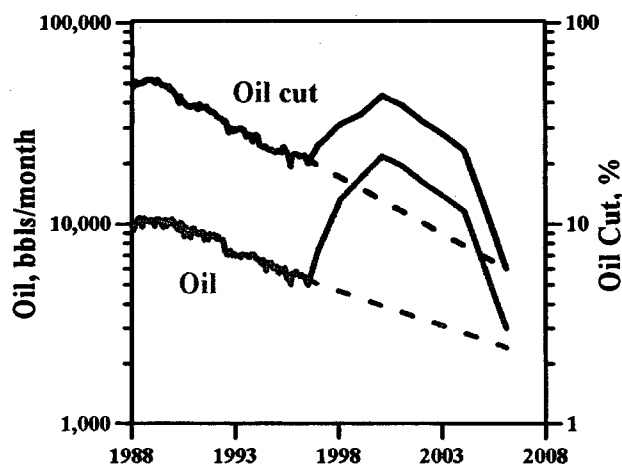


Fig. 1. Forecast of ASP and waterflood performance for a reservoir with 5.6 million bbl original oil in place indicates that ASP flooding would result in an additional 1.2 million bbl of oil.

participate in state-of-the-art chemical improved oil recovery.

Since chemicals are purchased throughout the injection of the first 0.5 pore volume or so, their cost is spread over half the life of the project, minimizing out-of-pocket expenses. If the field is currently producing at a high enough oil cut so that chemical costs are born by current oil production, then the cash flow is always positive. For instance, if the waterflood economic limit is at an oil cut of 2%, and if the field is producing at about 10% oil cut or greater, cash flow during ASP injection will be positive.

FIELD AND PILOT EXAMPLES

The response to ASP injection for a small oil reservoir with 5,595,000 bbl OOIP is shown in Fig. 1. The field has produced 1,460,000 bbl since discovery in 1973 and initiation of waterflooding in 1979. Continued waterflooding would produce an ultimate recovery of 44% OOIP with 518,000 bbl recovered in the 10 years from 1997 to 2007, when oil cuts decline from 21% to 7%.

Using ASP, the oil cut increases to 44% and an additional 1,200,000 bbl of oil is produced. The ASP solution is injected for 0.25 pore volume during the first four years followed by a tapered polymer flush. The total cost of the chemicals is \$2,625,000 with an additional \$200,000 in plant modification and design costs. Thus, the cost per incremental barrel of oil is \$2.35. Assuming a price of \$14 per bbl for this 20° API, high sulfur oil, the annual rate of return approaches 100% with a present worth of \$5,703,000 discounted at 10%.

The ASP process need not be limited to mature waterfloods. In fact, perhaps the most economical time to apply it is early in the project life. One reason is that the operational cost of the waterflood is not duplicated. If applied in a tertiary mode, a field may have a waterflood life of, for example, 30 years. Twenty-five years into the

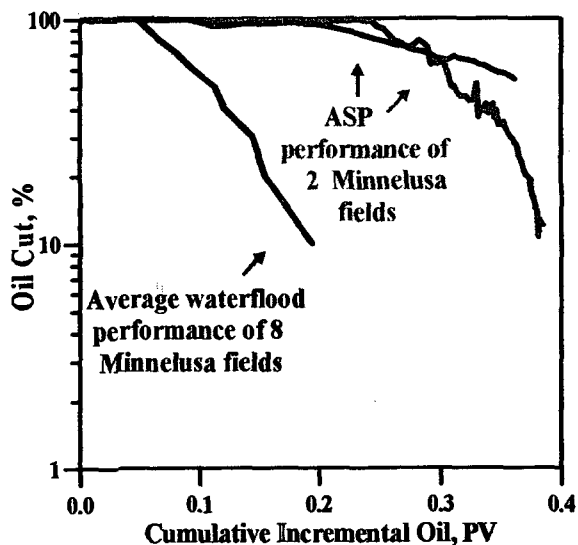


Fig. 2. Average waterflood performance of eight fields in the Powder River basin are compared to ASP floods in two similar fields. Primary oil recovery is not shown, only performance after fluids were injected.

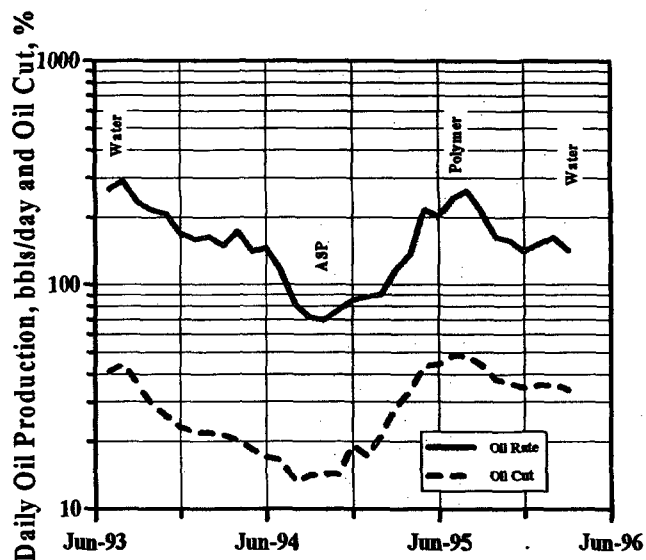


Fig. 3. Example of a tertiary application of ASP flooding was provided by a Daqing pilot test. Pilot was a 13-well, inverted 5-spot pattern.

waterflood, the ASP process is applied, which extends the reservoir life by five years, producing an extra 25% OOIP. But if the process had been applied early in the waterflood life, the extra oil and some of the waterflood oil would have been produced at higher oil cuts and the total project life would have been reduced significantly.

The performance of two actual ASP projects in the Powder River basin have been compared with the average of eight waterfloods in analogous reservoirs in the same area, Fig. 2.^{1,2} This plot shows only the performance after fluids are injected and not the primary oil recovery. Note that the average waterflood experiences water breakthrough after recovering about 0.06 pore volume of oil, whereas the ASP projects did not have a water breakthrough until about 0.20 pore volume of oil recovery. In fact, water breakthrough for the ASP projects occurred when the average of the waterfloods had declined to only about 10% oil cut. More than twice as much total fluid had to be injected in the waterflood to get to that point. Thus, the same oil recovery took less than half the time for the ASP projects.

The increased present worth of producing that oil in less than half the time as a waterflood more than pays for the chemicals. This is before any consideration is given to the additional 0.18 pore volume of incremental oil produced. Both ASP projects shown are quite economically successful. This was in spite of the fact that for one of the projects, oil prices

dropped below \$10 per bbl and averaged about \$12.50 per bbl for two years during ASP injection.

A more conventional philosophy is that the depletion would proceed through the primary, secondary, and tertiary stages. Certainly, this final tertiary stage holds significant promise for revitalizing mature waterfloods. A field example of this process in a tertiary application is the 1993 ASP pilot project in the Daqing oil field.³ This 13-well pilot contained four inverted 5-spot patterns. With this pattern, there are four injection wells, plus four corner, four side, and one central producing well. The central well is completely confined, and the side wells are each influenced by two injection wells.

The combined performance of the confined and four side wells is shown in Fig. 3. This pilot area is within a supergiant field that is under waterflood and which produces more than 1.1 million bpd of oil at oil cuts of about 25%. Thus, the pilot area had been partially waterflooded before the pilot test. This is evident from the average initial oil cuts of 40.9% when baseline waterflooding was initialized in July of 1993.

Water injection continued for 14 months before ASP injection, and the oil cuts had decreased to an average of 13.3%. The response was observed in all pilot area wells within 0.05 pore volume of ASP injection. In Fig. 3, oil cuts increased from 13.3% to 48.5% and production rate increased from 81 bpd to 262 bpd. The ASP pilot performance shows

that more than 25% OOIP of additional oil will be produced than would have from waterflooding.

A high capacity polyacrylamide polymer manufacturing plant, capable of producing 50,000 metric tons/year, was built in Daqing after successful polymer flood pilots. More than half the chemical cost for ASP flooding is that of the polymer. Yet, ASP technology recovers two to four times more incremental oil than will be recovered from polymer flooding alone. With the above pilot results and a polymer plant already in place, it is no surprise that the ASP pilot in Daqing is being extended.⁴

HOW ASP WORKS

The mechanisms of ASP technology are similar to that of the field proven, yet currently uneconomic, micellar polymer flooding. The major players in micellar research, including Shell, Texaco, Exxon, Phillips, Marathon, Union, etc., spent hundreds of millions of dollars in lab experiments and field trials in the 1970s and early 1980s proving the technology worked and would be economic when oil prices topped \$30 or more per bbl. Scientists and engineers involved with micellar technologies were able to recover 70% OOIP, or more, in some field trials with injection of less than 10% of a pore volume of a micellar slug followed by a mobility control buffer and water. These field trials were based on significant lab efforts to optimize the micellar design. The response validated the technology and

also the use of lab work to minimize the risk of applying the technology.

For the micellar technology, the primary mechanisms were: development of ultra-low interfacial tension and miscible displacement.⁵ The former mechanism affects the fractional flow and the latter affects phase behavior. Both of these mechanisms are ingrained in the ASP technology, although low interfacial tension is probably more significant. But the question is whether lowering the oil-water interfacial tension improves oil recovery efficiency?

It is the high interfacial tension between oil and water that

leads to the adage that oil and water do not mix. When oil is surrounded by water, this tension forms a sphere of oil in order to minimize the surface area exposed to the water. The oil drop behaves much like it is surrounded by an elastic film that can be distorted using force, but will return to spherical shape when the force is removed.

In waterflooding, water saturations are eventually reached when the oil drops and ganglia are discontinuous and no longer mobile. This is the waterflood endpoint of a relative permeability curve. These droplets are too large to fit through the pore throats in the rock matrix. It may be possible to push some of them through by applying enough force, but this is, of course, limited by parting pressure of the reservoir.

However, the droplets can be distorted if the interfacial tension is reduced, which is the purpose of the alkali and surfactant in the ASP solution. These two chemicals act synergistically, providing the ideal pH, ionic strength, and surfactant type to optimize the surfactant interactions at the oil-water interface.⁶ With properly designed ASP solutions, the interfacial tension can be reduced by three or more orders of magnitude, greatly increasing the efficiency of displacing the oil from the pores.

Once the interfacial tension is reduced, the droplets must be mobilized. The problem is that the aqueous solution may be more mobile than the oil, particularly as the water saturation increases. However, the water mobility can be reduced by adding polymer to increase the solution viscosity. In this manner, the

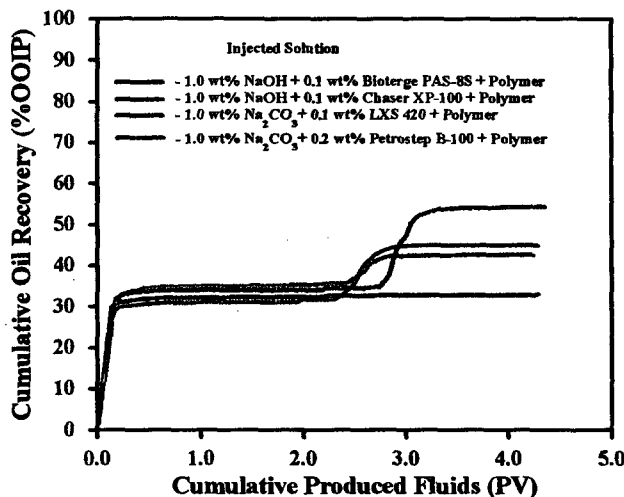


Fig. 4. Radial core flood performance of four ultra-low interfacial tension ASP systems with the same 42° oil and rock.

displaced oil can be pushed ahead of the advancing chemical solution. Furthermore, improving the mobility ratio has the added benefit of increasing the overall reservoir contact efficiency.

Lowering the interfacial tension does not guarantee that the oil will be displaced. Fig. 4 shows the performance of four radial core floods with 0.3 pore volume of ASP solution injected. All of these solutions produced ultra-low interfacial tension between the 42° API crude oil and surfactant solution of 0.001 dyne/cm or less. All had the same 500 mg/l polymer concentrations and polymer drive solution volume. But there was a wide range of response to the ASP solution, as can be seen from Fig. 4.

By using interfacial tension as a sole design criterion, one ignores the oil-rock and water-rock interfaces, phase behavior, effects of cation exchange from the rock and of chemical consumption. With all of these factors to consider, the lab effort to optimize the ASP solution can be significant, but much less costly than drilling a 4,000 ft well. Which engineer would not drill the well based upon a strong possibility of increasing reserves by 25% OOIP?

The ASP technology has a sound physical-mechanistic basis, has been field tested and has proven to be economically viable. The lab design, coupled with physical and numerical simulation, can reduce the risk of ASP technology in the same manner that 3-D seismic has reduced drilling risks. In this business there is always a benefit-risk parity; it is simply a matter of what type of risk one is comfortable taking. But the very nature of growth and of learning requires that new ideas

and opportunities be tested. Sometimes the finding is that it was not such a big risk after all. With ASP technology, one does not even need to find the oil; its location is already known, and generally speaking, so are the wells. Finding a way to produce it may be the best discovery ever.

Paper published in *WORLD OIL*/JULY 1997

THE AUTHORS

Kon Wyatt, project engineer with Surtek since 1980, is responsible for design and numerical simulation of waterfloods and chemical floods. Wyatt holds a BS degree in chemistry from Lewis and Clark College and an MS degree in mechanical engineering from Colorado School of Mines.

Malcolm J. Pitts is director of petroleum technology for Surtek in Golden, CO., where he has designed and numerically simulated chemical floods since 1980. He holds a BS degree in chemistry from the University of Colorado, an MS in bio-chemistry from Purdue University and a PhD in chemistry from Georgetown University.

Harry Surkalo is president of Surtek. He has been involved in chemical flooding for 30 years, beginning with micellar/polymer projects implemented by Marathon Oil in the 1960s. Surkalo holds a BS degree in petroleum engineering from Pennsylvania State University.

LITERATURE CITED

- Wyatt, K., Pitts, M., Surkalo, H., and Griffith, L.: "Alkaline-Surfactant-Polymer Technology Potential of the Minnelusa Trend, Powder River Basin," *SPE* 29565, 1995.
- Malcolm Pitts, Harry Surkalo and Kon Wyatt: "Design and Field Implementation of Alkaline-Surfactant-Polymer Chemical Enhanced Oil Recovery Systems," Proceedings of the 6th UNITAR International Conference on Heavy Crude and Tar Sands, Feb. 12-17, 1995, Houston TX.
- Gao, Shutang, Huabin Li and Zhenyu Yang, Institute of Petroleum E&D, Daqing Oil Field and Pitts, M.J., H. Surkalo and K. Wyatt, Surtek, Inc., "Alkaline-Surfactant-Polymer Pilot Performance of the West Central Saertu, Daqing Oil Field." *SPE Reservoir Engineering*, August 1996.
- Wang Demin, Jhang Zhenhua, Cheng Jiecheng, Yang Jingchun, Gao Shutang, Li Lin. "Pilot Test of Alkaline-Surfactant-Polymer Flooding in Daqing Oil Field," *SPE* 36748, 1996.
- Larson, R.G., H.T. Davis and L.E. Scriven, "Elementary Mechanisms of Oil Recovery by Chemical Methods," *Journal of Petroleum Technology*, Feb. 1982.
- Rudin, J. and D.T. Wasan, "Mechanisms for lowering of Interfacial Tension in Alkali/Acidic Oil Systems-2. Theoretical Studies," *Colloids and Surfaces*, 1992.

COPY

ASP Flood Raises Output

When primary production doesn't meet corporate needs, go after incremental oil with an alkaline-surfactant-polymer flood.

BY MALCOLM PITTS, KON WYATT AND HARRY SURKALO

Alkaline-surfactant-polymer (ASP) flooding is an advanced waterflood technology that, when applied early in the project life or later during waterflooding, produces 20% to 30% original oil in place incremental oil at costs from \$2/bbl to \$4.50/bbl. The economics of field projects can be examined and contrasted when ASP injection begins immediately after primary production and in a mature waterflood.

The 1.295 MMbbl pore volume West Kiehl Minnelusa ASP project in the Powder River Basin of Wyoming, performed in 1987, was the first full field ASP project. Pore volume is the space available in a reservoir to hold its oil, water, and gas. Minnelusa reservoirs routinely are waterflooded. However, the West Kiehl Reservoir, with 24° API crude oil, was flooded with an ASP solution after primary production. The project, initiated by Terra Resources, was purchased by Pacific Enterprises and finished by Hunt Oil.

More recently, the Daqing Petroleum Administrative Bureau performed a 1.279 MMbbl pore volume tertiary demonstration project of the ASP process. The project, initiated in September 1994 in the west center area of the Daqing Oil Field in northeastern China, began producing 35° API crude. Generalized waterflooding began in Daqing in 1960, with the ASP pilot waterflood beginning in 1993.

Economics

Additional costs associated with ASP technology come from the use of injected chemicals. With waterflooding, the plant must be modified for chemical storage and transfer, blending, filtration and possibly, water softening. These costs, however, are minor compared with the costs of injecting an ASP solution into 25% pore volumes, which costs about \$1 per injected barrel.

The economics depend upon many factors, including type, cost and concentration of chemicals; water treatment costs; injection rate; timing of the response; incremental oil recovery; and oil value. The West Kiehl and the Daqing projects contrast many of these variables.

The cost of the chemicals, capital improvements and design for the West Kiehl project was 35.1¢/bbl of pore volume. Chemicals represent 82% of these costs.

Costs for the Daqing project were estimated. The design cost assumes 1998 pricing; capital costs are five times the West Kiehl's costs. Chemical costs are higher because the surfactant concentration is three times greater, the alkali concentration is 47% greater, and the polymer concentration is 14% greater. Using US prices, these costs are estimated at 96.1¢/bbl of pore volume for Daqing. Here chemical costs were 67% of the total.

On the other hand, the value of the oil produced at West Kiehl is about \$3/bbl below Daqing crude because of its low gravity and high sulfur content. In both projects, the operating cost is borne by the existing waterflood, so there is no incremental operation cost.

West Kiehl and Daqing are on the extremes of the cost range for implementing the ASP technology. A total cost of about 50¢/bbl of treated pore volume is reasonable for estimation purposes. The larger the project, the greater fraction the chemical costs are of the total cost. Successful projects will recover 0.12 to 0.20 pore volumes of additional oil.

Numerical simulation established the West Kiehl incremental oil production greater than waterflooding. This incremental recovery of 197 Mbbl or 0.15 pore volume cost \$2.32/bbl, considerably less than the average U.S. oil replacement cost of \$5.26/bbl, according to Arthur Andersen's "1997 Oil and Gas Reserve Disclosure." Using the Wyoming average yearly oil price less \$3, ranging from \$10.50 in 1988 to \$18 in 1990, the actual yearly costs for the ASP project and the incremental oil recovery permit calculating the economics of the West Kiehl project. The annual rate of return for the ASP project investment is 83%, providing a 10% discounted present worth of \$1.03 million.

Estimating the Daqing waterflood recovery based on numerical simulation results in 199 Mbbl or 0.155 pore volume of incremental oil. Using West Texas Intermediate average yearly oil prices, the estimated yearly costs and the actual oil recovery less the simulated waterflood oil recovery provides a rate of return greater than 100% and a 10% discounted present worth of \$1.27 million.

Figure 1 compares the cumulative cash flow for the West Kiehl and Daqing ASP projects. The West Kiehl design costs and the purchase of some of the chemicals were

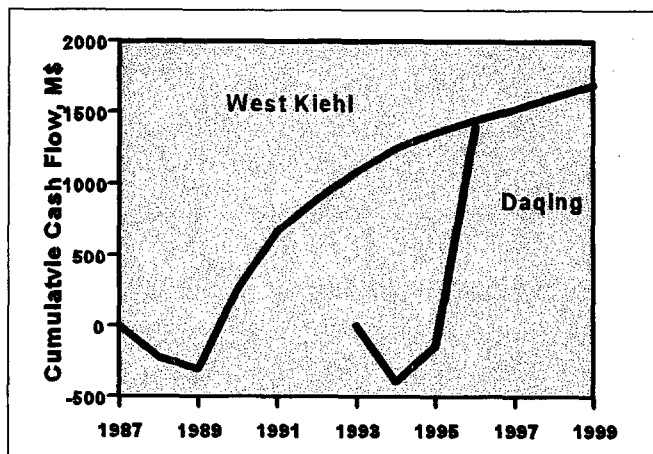


Figure 1. Cumulative cash flow of incremental ASP costs for West Kiehl and Daqing.

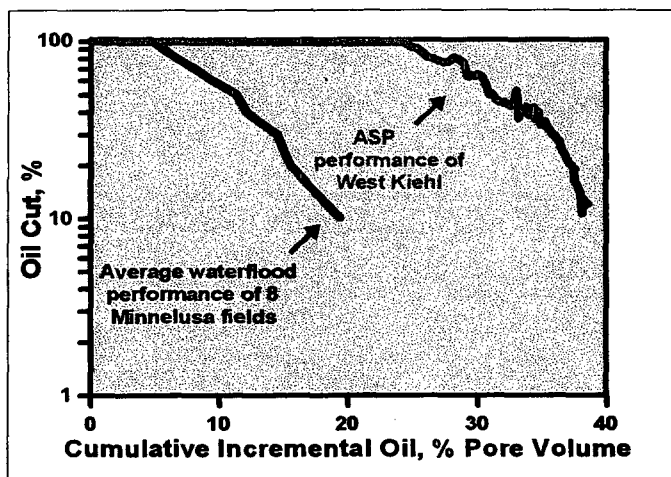


Figure 2. Average Minnelusa waterflood and West Kiehl performance.

made in 1987 with ASP injection beginning in 1988. The project paid out in 2.5 years, and by April 1990, the cumulative cash flow for the ASP project was greater than for the simulated waterflood.

The Daqing ASP project, performed in a pilot area with nine production wells and four injection wells, used the same wells as an earlier polymer flooding pilot in a deeper producing horizon. Because of the number of wells in the small pore volume, this project was completed in about three years compared with the 10 years for West Kiehl. Naturally, this enhances the economics. Thus, even with 2.72 times greater costs per barrel of pore volume for Daqing, the economics were similar. As with waterflooding, drilling additional wells may accelerate the project and enhance the economics.

Performance

The performance of the West Kiehl Field compared with the average of eight analogous Minnelusa waterfloods is shown in Figure 2. This figure shows only the oil recovery after fluids were injected and does not include primary production. The average waterflood breakthrough occurs after recovering about 6% pore volume of oil. The West Kiehl project did not experience water breakthrough until about 20% pore volume was injected, when the average waterflood had an oil cut of 10%. The average waterflood, with lower oil cuts, required much more injection to get to 20% pore volume oil recovery. This significantly increased the present worth, with no consideration given to the additional 18% pore volumes of oil greater than the average waterflood that the West Kiehl produced.

In the Daqing ASP pilot with the simulated waterflood, oil cuts increased from 11.6% to 31.2%, with a roughly twofold increase in oil production rate. For the central confined production well, the oil rates increased sevenfold with oil cuts increasing from 13% to 51.4%.

Requirements

As with all ASP projects, the West Kiehl and Daqing are good waterflood candidate reservoirs. Because each reservoir has unique oil, water, and rock characteristics, the solutions

designed for injection are also unique. Laboratory studies screen low cost, commercially available alkali, surfactant, and polymers to determine formulations that reduce the capillary forces trapping the waterflood residual oil and efficiently displace it. Coreflood evaluations physically simulate the process in a reservoir core at reservoir conditions to optimize the formulations and verify the incremental oil recoveries. These laboratory studies determine if the ASP technology is amenable for a particular reservoir. Often numerical simulation studies are performed to estimate the field performance and economics.

Not all waterfloods are amenable to the ASP technology. The water used to blend the chemicals must be low in hardness or economical to soften. Temperatures higher than 210°F may affect chemical stability. Aside from these, most limitations are economical rather than technical. To provide rates of return of 40% or greater, injection rates of one pore volume in 15 years or less are desired.

The oil industry constantly strives for new technologies to reduce cost, save time, and improve recovery. We tend to observe the risks taken by others critically, to determine if they were justified economically or technically. Unlike many of the recently proven technologies, chemical floods may take a few years to respond and decades to complete. They are not a quick fix for an ailing reservoir, but may be a means to produce some of the otherwise abandoned resource. The field results of the early ASP projects performed by those who took the risk in this technology show the projects have been successful economically and technically.

There are currently 2 other Minnelusa ASP projects ongoing, 2 others planned for startup in 1998, and several in the initial design stage. A dolomite project in Texas is scheduled for 1998. The Daqing ASP project has been expanded. There are at least 3 other ASP projects in China. Argentina is likely to see its first ASP project in 1998. Universally, the goal is to add additional reserves from an existing resource, a resource that is becoming more expensive and difficult to reach by conventional methods.

A shortened version of this paper was published in *the OIL and GAS WORLD*/March 1998

About the Authors

Malcolm J. Pitts is director of petroleum technology for Surtek Inc. in Golden CO., where he has designed and numerically simulated chemical floods since 1980. He is the Rocky Mountain region director for the Society of Petroleum Engineers.

Kon Wyatt, project engineer with Surtek since 1980, is responsible for design and numerical simulation of waterfloods and chemical floods.

Harry Surkalo is president of Surtek. He has been involved in chemical flooding for 30 years, beginning with micellar-polymer projects implemented by Marathon Oil in the 1960's.

From: pitts@surtek.com
Date: Wednesday, May 28, 2003 10:15:04
To: bmg@digii.net
Subject: [Fwd: Darsh Wasan's Nature article]

COPY

Al:

I talked to Dr. Wasan about his research with surfactants discussed in the Science News article you sent us. Very interesting! A copy of the Nature article is attached. Darsh mentioned that he believes in a fractured reservoir such as you have that the mechanism he saw in the lab could apply. His research shows that to lift oil off a surface that surfactant micelles ("nanofluids") provide a wedge between the solid matrix and the attached oil drop. To take advantage of this mechanism for the East Puerto Chiquito Mancos Unit, we need to maintain surfactant concentrations above the critical micelle concentration for as long as possible. So, in the laboratory work we need to look at 0.2, 0.3 wt% surfactant.

How do you stand on the Estrada water? For the laboratory work, we will need about 15 gallons. Also, we will need some new oil, about 10 gallons, and new produced water, about 15 gallons.

Sincerely,
 Malcolm Pitts
 SURTEK

----- Original Message -----

Subject: Darsh Wasan's Nature article
Date: Fri, 23 May 2003 14:18:05 -0500
From: Judith Ackerman <ackerman@iit.edu>
To: pitts@surtek.com

file
 SURTEK METHOD
 CC: Mike, Tom, Jim, Susan

05/28/2003

letters to nature

18. Plesset, M. S. & Prosperetti, A. Bubble dynamics and cavitation. *Annu. Rev. Fluid Mech.* **9**, 145–185 (1977).
19. Leighton, T. G. *The Acoustic Bubble* (Academic, London, 1994).
20. Lighthill, J. Acoustic streaming. *J. Sound Vib.* **61**, 391–418 (1978).
21. Miller, D. L., Nyborg, W. L. & Whitcomb, C. C. Platelet aggregation induced by ultrasound under specialized conditions. *Science* **205**, 505–507 (1979).
22. Miller, D. L. Particle gathering and microstreaming near ultrasonically activated micropores. *J. Acoust. Soc. Am.* **84**, 1378–1387 (1988).
23. Elder, S. A. Cavitation microstreaming. *J. Acoust. Soc. Am.* **31**, 54–64 (1958).
24. Davidson, B. J. & Riley, N. Cavitation microstreaming. *J. Sound Vib.* **15**, 217–233 (1971).
25. Rooney, J. A. Hemolysis near an ultrasonically pulsating gas bubble. *Science* **169**, 869–871 (1970).
26. Longuet-Higgins, M. S. Viscous streaming from an oscillating spherical bubble. *Proc. R. Soc. Lond. A* **454**, 725–742 (1998).
27. Blake, J. R. & Chwang, A. T. Fundamental singularities of viscous flow. *J. Eng. Math.* **8**, 23–29 (1974).
28. Pozrikidis, C. *Boundary Integral and Singularity Methods for Linearized Viscous Flow* (Cambridge Univ. Press, Cambridge, UK, 1992).
29. Riley, N. On a sphere oscillating in a viscous fluid. *Q. J. Mech. Appl. Math.* **19**, 461–472 (1966).
30. Seifert, U. Fluid membranes in hydrodynamic flow fields: Formalism and an application to fluctuating quasispherical vesicles in shear flow. *Eur. Phys. J. B* **8**, 405–415 (1999).

Supplementary Information accompanies the paper on www.nature.com/nature.

Acknowledgements We thank D. Lohse for his support and insight, and A. van den Berg and H. Gadeniers for discussions.

Competing interests statement The authors declare that they have no competing financial interests.

Correspondence and requests for materials should be addressed to P. M. (p.marmottant@tn.utwente.nl).

Spreading of nanofluids on solids

Darsh T. Wasan & Alex D. Nikolov

Department of Chemical and Environmental Engineering, Illinois Institute of Technology, Chicago, Illinois 60616, USA

Suspensions of nanometre-sized particles (nanofluids) are used in a variety of technological contexts. For example, their spreading and adhesion behaviour on solid surfaces can yield materials with desirable structural and optical properties¹. Similarly, the spreading behaviour of nanofluids containing surfactant micelles has implications for soil remediation, oily soil removal, lubrication and enhanced oil recovery. But the well-established concepts of spreading and adhesion of simple liquids do not apply to nanofluids^{2–7}. Theoretical investigations have suggested that a solid-like ordering of suspended spheres will occur in the confined three-phase contact region at the edge of the spreading fluid, becoming more disordered and fluid-like towards the bulk phase^{8,9}. Calculations have also suggested that the pressure arising from such colloidal ordering in the confined region will enhance the spreading behaviour of nanofluids^{10,11}. Here we use video microscopy to demonstrate both the two-dimensional crystal-like ordering of charged nanometre-sized polystyrene spheres in water, and the enhanced spreading dynamics of a micellar fluid, at the three-phase contact region. Our findings suggest a new mechanism for oily soil removal—detergency.

When a gas bubble or oil/liquid drop dispersed in an aqueous nanofluid approaches a smooth, horizontal hydrophilic solid surface, there is a microscopic transition between the liquid film and the meniscus—and the nanofluid film can change its thickness in steps¹¹. The transition region between the liquid film on a solid surface and the bulk meniscus has a wedge-like profile (Fig. 1), and its shape is determined by forces arising from the ordering of particles or supermolecules, such as surfactant micelles. Structural transitions have been observed in colloidal fluids confined to very thin wedges^{12–15}.

The aim of this study is to reveal the effects of the particle

structure formation and the structural disjoining pressure on the spreading of colloidal fluids on solid surfaces. Spreading is generally described in terms of the spreading coefficient S , given by $S = \sigma_{sg} - \sigma_{sl} - \sigma_{lg}$, where σ is the respective interfacial tension existing between the solid–gas (σ_{sg}), solid–liquid (σ_{sl}) and liquid–gas (σ_{lg}) phases. The de Gennes theory relates the value of S to the disjoining pressure of a wetting film ($\Pi(h)$, where h is the thickness of the film) as^{2,16}:

$$S = \Pi(h)h + \int_h^{\infty} \Pi(h) dh \quad (1)$$

We directly observed the particle-structuring phenomenon in the liquid film–meniscus region by using reflected-light digital video microscopy. The wedge film was formed by blowing a small air bubble (diameter 200 μm) against an optically smooth glass plate in a suspension of monodisperse, charged latex spheres in deionized surfactant-free water. The volume fraction of spheres in the fluid

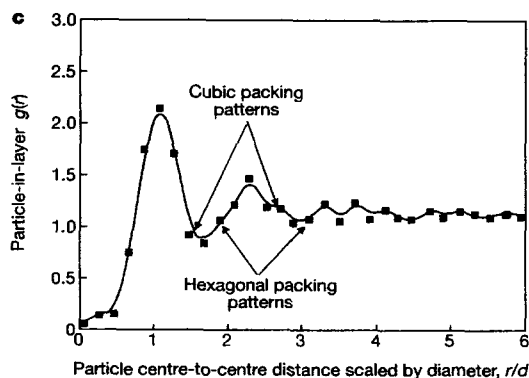
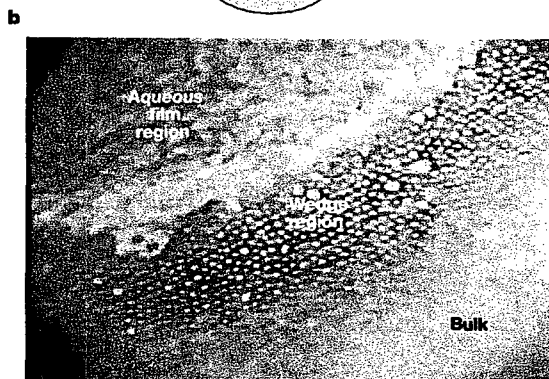
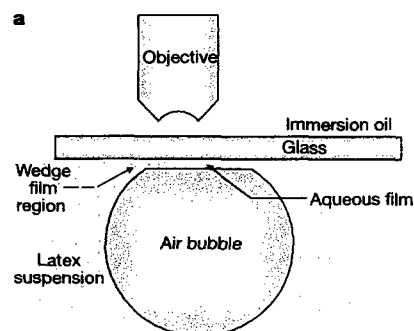


Figure 1 Particle structuring in a wedge film. **a**, Diagram of experimental set-up. **b**, Particle structuring in a wedge film. Latex particles had diameter 1 μm , charge $0.8 \mu\text{C cm}^{-2}$, and occupied 7 vol.%. **c**, In-layer particle structure inside the wedge film. Mean particle-to-particle distance was 1.2 d , effective particle volume was 44 vol.%.

was 7 vol.%, and they had a surface charge of $0.8 \mu\text{C cm}^{-2}$, a diameter of $1.01 \mu\text{m}$, and a density of 1.05 g cm^{-3} . Figure 1a shows a diagram of the experimental set-up. Special precautions were taken to eliminate light coming from the air-bubble/liquid surface as well as light reflected from the glass/air surface and heating effects. The optical signal was digitized for analysis. Figure 1b shows a photomicrograph taken in reflected light depicting the formation of a two-dimensional (2D), in-layer, colloidal crystal structure in the three-phase contact region (that is, in the wedge film). The latex particles tend to form a 2D colloid crystal structure at a thickness of the wedge film equal to twice the particle diameter (that is, about $2 \mu\text{m}$). However, the particle in-layer structure changes to a disordered structure when the film thickness exceeds three particle diameters (see Supplementary Information movie 1). The co-existence of this ordered-disordered structure depicted in Fig. 1b is reproducible, and was observed for several hours.

Figure 1c shows the particle in-layer radial distribution function, $g(r)$, that we obtained from the image analysis of over 2,000 particles. This figure shows the co-existence of both the 2D hexagonal and cubic packing domains in the wedge film.

We also used computer-enhanced video microscopy to monitor the position of the particle oscillations in the three-phase contact region (Supplementary Information movie 1). The brownian motion of the colloidal latex particles along the x and y axes were measured in more than 600 successive time intervals of 0.033 s. The period of oscillation was about 2 Hz. Plots of the probability density distribution function for the disordered and ordered particle structures are shown in Fig. 2a and b, respectively. The results

show that the particle displacements due to brownian motion follow a gaussian distribution. However, we note that the particle mean-square displacement (standard deviation) for the ordered and disordered structures is very different. The value of the mean-square displacement for the 2D colloidal crystal-like structure is $0.17d$ (where d is particle diameter) compared to $0.9d$ for the random-packed structure. The mean interparticle distance is $1.2d$.

We also estimated the energy of interaction between the particles in the three-phase contact region using the Boltzmann equation. The energy for particle crystallization (that is, changing particles from a random-packed structure to a 2D colloid crystal-like structure) was calculated to be only $1.8kT$ (where k is the Boltzmann constant, and T is temperature). The particle-particle mean interaction potential becomes oscillatory owing to the particle crystallization in the wedge film, so the film disjoining pressure (Π) versus film thickness (h) has an oscillatory decay.

In Fig. 3a we plot disjoining pressure, obtained by using an analytical expression based on statistical mechanics¹⁰. The pressure is high (nearly 50,000 Pa) near the vertex, because the hard spheres are 'pushed' into the region by the spheres farther out. The pressure oscillates as 1, 2, 3 and 4 layers of hard spheres can be accommodated between the wedge confinement, and ultimately becomes the bulk hard-sphere pressure. The magnitude of this pressure depends on the effective particle volume fraction and particle size. We confirmed these integral equation results by comparison with Monte Carlo simulation results⁸. Computer simulations have shown that there is a tendency for the spheres near the vertex to have a solid-like structure, and for those further from the vertex to have a fluid-like structure^{8,9}. These theoretical results confirm our experimental observations on the particle structure formation in the wedge film (Fig. 1).

The spreading coefficient, S , was estimated as a function of the number of particle layers in the wedge film using equation (1) and the analytical expressions derived from the Ornstein-Zernike

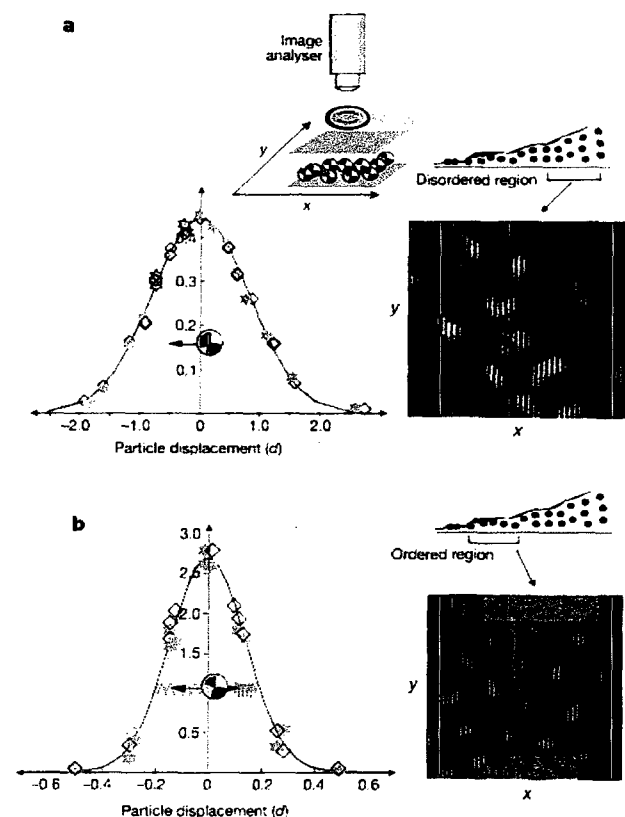


Figure 2 Distribution of particle displacement inside the wedge film. **a**, Inside the 2D random packing region; **b**, inside the 2D 'crystal' region. In graphs, stars and diamonds show respectively x and y displacements. Video prints show instantaneous particle positions.

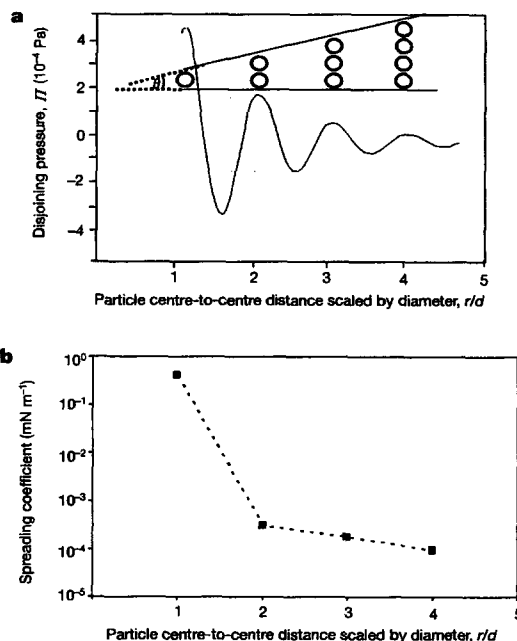


Figure 3 Pressure profile and spreading coefficient as a function of film thickness. **a**, Pressure profile on the wedge walls as a function of film thickness r scaled by particle diameter d . Particle volume fraction, 0.4; particle diameter $d = 8 \text{ nm}$. **b**, Spreading coefficient arising owing to particle disjoining pressure. Nanofluid properties as in **a**.

equation for the structural disjoining pressure in the film¹⁰ (Fig. 3a). Our calculations show that the spreading coefficient increases with a decrease in film thickness, that is, with the decrease in the number of particle layers inside the film (Fig. 3b). Also, we notice a significant change in the slope of the curve at a thickness of the wedge film equal to twice the particle diameter. Our Monte Carlo simulations showed that at this film thickness the particle in-layer structure changes to an ordered structure¹¹. These results indicate that the in-layer particle structuring can enhance the spreading of nanofluids on solids.

Next, we studied the spreading dynamics of micellar fluids and role of the structural component of the disjoining pressure arising from the nanoparticle (micelle) ordering inside the film-meniscus region (that is, the wedge film) in the oily soil removal process. We studied the oil/solid interactions in the presence of an aqueous micellar solution, using differential and common three-phase contact angle interferometry^{17–22}. Figure 4a shows the interference patterns produced by an oil droplet (of volume 10 μl) on a glass/air surface observed by reflected light using a differential microscope (Supplementary Information movie 2). The interference patterns seen in this photomicrograph as parallel, regular, continuous lines depict the topology of the wedge film region. The distance between the patterns and their order of interference can be used to calculate the local radii of curvature. These radii, in conjunction with the surface tension data, allow us to calculate the capillary pressure. We can construct the surface plot of the three-phase contact region using the interference patterns.

The sequence of photographs shown in Fig. 4b–e depict the three-phase contact angle dynamics and the various steps of oil droplet removal from the glass surface in the presence of an aqueous micellar solution. (The solution consisted of anionic sodium lauryl sulphate surfactant of an effective micelle diameter of 8 nm, and at a concentration equal to ten times the critical micelle concentration, that is, an effective volume fraction of 0.4, or a concentration of 0.1 mol l⁻¹). We see that the micellar solution penetrates between the oil and the glass surface (Supplementary Information movie 3). The speckled band between the dark and light areas in Fig. 4b and c shows the formation of small aqueous lenses (seen as the white spots

encircled by dark fringes) between the oil and solid surface. In effect, two contact regions are established: the first is between the oil droplet, the solid surface and the aqueous surfactant solution (outer region), and the second is between the oil droplet, the solid surface and the aqueous film with lenses (inner region). A pre-wetted aqueous film with lenses is formed between the two regions. The thickness of the speckled band increases with the lapse of time, because the inner contact region recedes more rapidly than the outer contact line (Fig. 4d). Eventually, the oil droplet is separated completely from the solid surfaces by a thick aqueous film with a dimple (Fig. 4e).

Our explanation for the detachment of an oil drop from the solid surface using a surfactant micellar solution (without an added electrolyte) is that with the lapse of time, micelles diffuse into the wedge film and interact with the film surfaces. The micelle concentration in the film increases. The disjoining pressure increases significantly at a wedge thickness corresponding to one micelle layer (Fig. 3a). As a result of the pressure increase, the oil–solution interface moves forward, and the aqueous micellar solution spreads on the solid surface, detaching the oil drop.

We performed an additional experiment to test the role of micellar interactions in the oil detachment process. In this experiment, we observed the separation of an oil drop from the glass surface in the presence of the same ionic surfactant but with an added electrolyte (0.1 mol l⁻¹ NaCl). However, the drop did not become detached from the solid surface. This was unexpected, because the interfacial tension at the interface between the oil and the aqueous micellar solution decreases at a higher salt concentration and, as a result, the droplet shrinks (Supplementary Information movie 4). This reduction in interfacial tension should have enhanced the separation process. In fact, at high salt concentrations, the effective micellar diameter (and thereby the micelle volume fraction) decreases, owing to the shrinkage of the electrical double layer around each micelle. Therefore, the magnitude of the structural disjoining pressure diminishes, thus reducing the driving force for the detachment of the drop. Further investigation is underway to elucidate the possible effects of salt concentration, micellar concentration and type, and micelle size and polydispersity on the role of

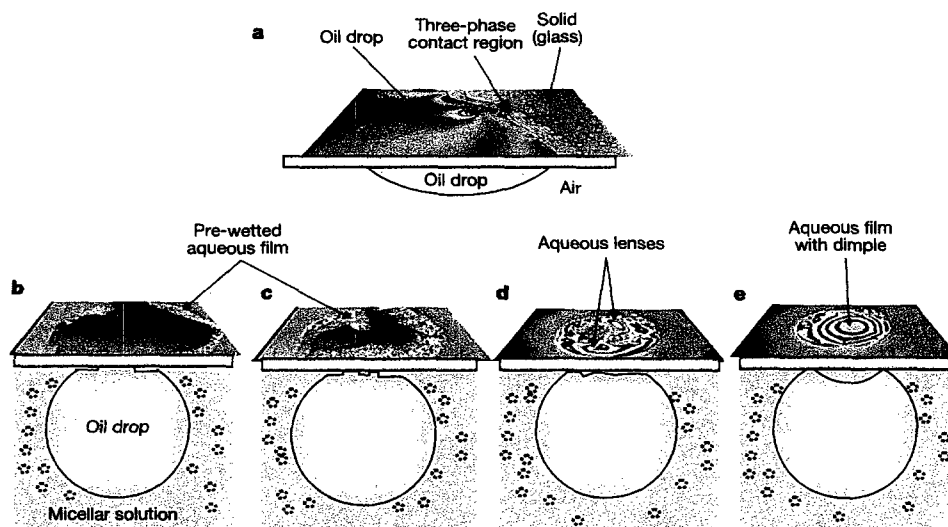


Figure 4 Dynamics of the three-phase contact region. **a**, Photomicrograph showing the oil drop placed on a glass surface and differential interference patterns formed at the three-phase (solid–liquid–air) contact region. **b–e**, Photomicrographs taken at increasing times after addition of the aqueous micellar solution: **b**, 30 s; **c**, 2 min; **d**, 4 min; and **e**, 6 min. **b**, The beginning of the formation of the pre-wetting aqueous

film between the glass surface and the oil droplet. **c**, The spreading of the pre-wetting film. **d**, The pre-wetted film now covers the whole area, and small water lenses are formed. **e**, The separation of oil droplet from the glass surface by a thick aqueous film with a dimple.

the structural disjoining pressure arising from the confined micelles in the oily soil removal process. □

Received 17 December 2002; accepted 21 March 2003; doi:10.1038/nature01591.

- Brauman, J. I. & Szuromi, P. Thin films. *Science* **273**, 855 (1996).
- de Gennes, P. G. Wetting: statics and dynamics. *Rev. Mod. Phys.* **57**, 827–863 (1985).
- Churaev, N. V. On the forces of hydrophobic attraction in wetting films of aqueous solutions. *Colloids Surf. A* **79**, 25–31 (1993).
- Ruckenstein, E. Effect of short-range interactions on spreading. *J. Colloid Interface Sci.* **179**, 136–142 (1996).
- Churaev, N. V. *et al.* The superspreading effect of trisiloxane surfactant solutions. *Langmuir* **17**, 1338–1348 (2001).
- De Coninck, J., de Ruijter, M. I. & Voué, M. Dynamics of wetting. *Curr. Opin. Colloid Interface Sci.* **6**, 49–53 (2001).
- Cazabat, A. M., Fraysse, N. & Heslot, F. The wetting films. *Colloids Surf.* **52**, 1–8 (1991).
- Boda, D., Chan, K. Y., Henderson, D., Wasan, D. T. & Nikolov, A. D. Structure and pressure of a hard sphere fluid in a wedge-shaped cell or meniscus. *Langmuir* **15**, 4311–4313 (1999).
- Tata, B. V. R., Boda, D., Henderson, D., Nikolov, A. D. & Wasan, D. T. Structure of charged colloids under a wedge confinement. *Phys. Rev. E* **62**, 3875–3881 (2000).
- Trokhymchuk, A., Henderson, D., Nikolov, A. D. & Wasan, D. T. A simple calculation of structural and depletion forces for fluids/suspensions confined in a film. *Langmuir* **17**, 4940–4947 (2001).
- Wasan, D. T. & Nikolov, A. D. in *Supramolecular Structure in Confined Geometries* (eds Marne, G. & Warr, G.) 40–53 (ACS Symposium Series Series No. 736, American Chemical Society, Washington DC, 1999).
- Pieranski, P., Stezleski, L. & Pansu, B. Thin colloidal crystals. *Phys. Rev. Lett.* **50**, 900–903 (1983).
- Pieranski, P. Colloidal crystals. *Contemp. Phys.* **24**, 25–73 (1983).
- van Winkel, D. H. & Murray, C. A. Layering in colloidal fluids near a smooth repulsive wall. *J. Chem. Phys.* **89**, 3885–3891 (1988).
- Murray, C. A. & Gier, D. Colloidal crystals. *Am. Sci.* **83**, 238–245 (1995).
- Neimark, A. V. & Kornev, K. G. Classification of equilibrium configurations of wetting films on planar substrates. *Langmuir* **16**, 5526–5529 (2000).
- Kao, R. L., Wasan, D. T., Nikolov, A. D. & Edwards, D. A. Mechanisms of oil removal from a solid surface in the presence of anionic micellar solutions. *Colloids Surf.* **34**, 389–398 (1989).
- Dimitrov, A. S., Kralchevsky, P. A., Nikolov, A. D. & Wasan, D. T. Contact angles of thin liquid films—interferometric determination. *Colloids Surf.* **47**, 299–321 (1990).
- Lobo, L. A., Nikolov, A. D., Dimitrov, A. S., Kralchevsky, P. A. & Wasan, D. T. Contact angle of air bubbles attached to an air/water surface in foam applications. *Langmuir* **6**, 995–1001 (1990).
- Nikolov, A. D., Kralchevsky, P. A., Ivanov, I. B. & Dimitrov, A. S. in *Thin Liquid Film Phenomena* (eds Krantz, W. B., Wasan, D. T. & Jain, R. K.) 82–87 (Symposium Series No. 252, Vol. 82, American Institute of Chemical Engineers, 1986).
- Nikolov, A. D., Dimitrov, A. S. & Kralchevsky, P. A. Accuracy of the differential–interferometric measurements of curvature—experimental study with liquid drops. *Opt. Acta* **33**, 1359–1386 (1986).
- Nikolov, A. D. & Wasan, D. T. in *Handbook of Surface Imaging and Visualization* (ed. Hubbard, A.) 209–214 (CRC, Boca Raton, Florida, 1995).

Supplementary Information accompanies the paper on www.nature.com/nature.

Acknowledgements This work was supported by the National Science Foundation.

Competing interests statement The authors declare that they have no competing financial interests.

Correspondence and requests for materials should be addressed to D.T.W. (wasan@iit.edu).

Redistribution of energy available for ocean mixing by long-range propagation of internal waves

Matthew H. Alford

Applied Physics Laboratory and School of Oceanography, University of Washington, 1013 NE 40th Street, Seattle, Washington 98105, USA

Ocean mixing, which affects pollutant dispersal, marine productivity and global climate¹, largely results from the breaking of internal gravity waves—disturbances propagating along the ocean's internal stratification. A global map of internal-wave dissipation would be useful in improving climate models, but would require knowledge of the sources of internal gravity waves and their propagation. Towards this goal, I present here

computations of horizontal internal-wave propagation from 60 historical moorings and relate them to the source terms of internal waves as computed previously^{2,3}. Analysis of the two most energetic frequency ranges—near-inertial frequencies and semidiurnal tidal frequencies—reveals that the fluxes in both frequency bands are of the order of 1 kW m^{-1} (that is, 15–50% of the energy input) and are directed away from their respective source regions. However, the energy flux due to near-inertial waves is stronger in winter, whereas the tidal fluxes are uniform throughout the year. Both varieties of internal waves can thus significantly affect the space-time distribution of energy available for global mixing.

The Earth's meridional overturning circulation (MOC), wherein millions of cubic metres of water sink each second at high latitude and upwell at low, is a vital element of ocean circulation and a key indicator of climate change in models⁴. Theory, profile fits and inverse models of ocean circulation^{5,6} suggest that the MOC requires of the order of 2 TW ($= 2 \times 10^{12} \text{ W}$) of power (though some argue for less⁷) to turbulently warm the abyssal waters so they can upwell. Breaking of internal gravity waves is thought to fuel this turbulence. Sufficient power appears to be available from the combined effects of the wind and the tides^{2,3,5,8,9}, but neither the partitioning of mixing between these sources, nor the energy pathways and resultant mixing distributions, are yet known. Direct measurements^{1,10,11} suggest that abyssal mixing is weak over much of the oceans, but spatially variable. Resolution of these issues is a major goal of physical oceanographers because climate models cannot resolve these processes, but are sensitive to both the magnitude and distribution of the resultant mixing¹². However, directly measuring mixing at all locations is not practical, so another approach is sought here.

Internal gravity waves occupy a frequency range bounded below by the local inertial frequency, $f \equiv 2 \sin(\text{latitude})$ cycles per day. By far the most energetic are 'near-inertial' waves, with frequencies $\omega \approx f$, and internal tides, at the astronomical frequencies (dominantly the semidiurnal M_2). The former are primarily generated by sudden wind events^{9,13} (and, to an unknown degree, by geostrophic adjustment at eddies and fronts); the latter by depth-independent tidal flow over sloping topography.

The energy inputs, S_f and S_{M_2} , into each type of motion vary substantially over the globe. Near-inertial energy input peaks during local winter near storm tracks (western mid-latitudes of each ocean), with a global total of 0.5 TW (ref. 3). This energy is initially input at $\omega \approx f$ into the ocean's surface layer, but models¹⁴ and observations^{15,16} show that deeper disturbances are quickly excited that propagate downward and equatorward towards lower f . The energy available for the M_2 internal tide is maximum near sloping topography, and has a total of 0.7 TW (ref. 2). Together with 1 TW of lower-frequency wind input⁸, there appears to be enough power to provide the 2 TW needed for abyssal stratification maintenance.

If waves did not propagate far, all mixing would occur near the sources. However, internal tides can be observed from space^{17,18} propagating thousands of kilometres from sources. Theory^{19,20} and circumstantial evidence¹⁶ suggest that near-inertial waves can also propagate a long way. Here I address the question 'how much does long-range propagation cause internal-wave dissipation distributions to differ from the sources?' In a steady ocean with perfect knowledge of the sources, $S(\mathbf{x})$, and of the subsequent horizontal energy flux by propagation, $F(\mathbf{x})$, internal-wave dissipation $D(\mathbf{x})$ is given by:

$$D(\mathbf{x}) = S(\mathbf{x}) - \nabla \cdot F(\mathbf{x}) \quad (1)$$

where \mathbf{x} is position. F is computed here in each frequency band at 60 discrete locations, using historical moored records and climatological profiles²¹ (Fig. 1, Methods), and compared to previously computed source distributions for each.